International Energy Agency

Heat, Air and Moisture Transfer in Insulated Envelope Parts

Design parameters used to avoid interstitial condensation for a range of climates

Report Annex 24, Task 2
Environmental conditions

Energy Conservation in Buildings and Community Systems Programme

INTERNATIONAL ENERGY AGENCY
Energy Conservation in Buildings and Community Systems

IEA ANNEX 24
Heat, Air and Moisture Transfer through new and retrofitted Insulated Envelope Parts (Hamtie)

Task 2
ENVIRONMENTAL CONDITIONS

DESIGN PARAMETERS USED TO AVOID INTERSTITIAL CONDENSATION FOR A RANGE OF CLIMATES

C.H. Sanders
BRE Scottish Laboratory
East Kilbride, UK

CONTENTS

PREFACE

DESIGN PARAMETERS USED TO AVOID INTERSTITIAL CONDENSATION FOR A RANGE OF CLIMATES

1. Introduction
2. The test reference years and construction parameters used
3. Factors affecting the pivot values derived by CLIMCHCK
4. Effect of different climates
5. Estimation of pivot values from monthly mean data
6. Effective pivot values
7. Allowable moisture generation rates
8. Geographical distribution of pivot values
9. Conclusions
10. References

Tables and Contour Maps

PREFACE

THE INTERNATIONAL ENERGY AGENCY

The International Energy Agency (IEA) was established in 1975 within the framework of the Organisation for Economic Cooperation and Development (OECD) to implement an International Energy Programme. A basic aim of the IEA is to foster cooperation among the 22 IEA Participating Countries to increase energy security through energy conservation, development of alternative energy sources and energy research, development and demonstration (RD&D). This is achieved in part through a programme of collaborative RD&D consisting of 42 Implementing Agreements, containing a total of over eighty separate energy RD&D projects.

ENERGY CONSERVATION IN BUILDING AND COMMUNITY SYSTEMS

As one element of the Energy Programme, the IEA sponsors research and development in a number of areas related to energy. In one of these areas, "Energy conservation in buildings and community systems", the IEA is backing various exercises to predict more accurately the energy use of buildings, including comparison of existing computer programmes, building monitoring, comparison of calculation methods, energy management systems as well as air quality and inhabitants behaviour studies. Eighteen countries and the European Community,

BELGIUM, CANADA, CEC, DENMARK, GERMANY, FINLAND, FRANCE, GREECE, ITALY, JAPAN, NETHERLANDS, NEW ZEALAND, NORWAY, POLAND (associate member), SWEDEN, SWITZERLAND, TURKEY, U.K., U.S.A.

have elected to participate and have designed contracting parties to the Implementing Agreement, covering collaborative research in this area. This designation by the government of a number of private organisations as well as universities and government laboratories as contracting parties, has provided a broader range of expertise to tackle the projects in the different technology areas than would have been the case if participation was restricted to governments. The importance of associating industry with government sponsored energy RD&D is recognised in the IEA, and every effort is made to encourage this trend.

THE EXECUTIVE COMMITTEE

Overall control of the programme is maintained by an Executive Commitee, which not only monitors existing projects but also identifies new area where collaborative effort may be beneficial. The Executive Committee ensures all projects to fit into a predetermined strategy without unnecessary overlap or duplication but with effective liaison and communication. Thirty projects have been initiated by the Executive Committee, of which the greater part has been completed:

ANNEX 1: Load energy determination of buildings (*)
ANNEX 2: Ekistics & advanced community energy systems (*)
ANNEX 3: Energy conservation in residential buildings (*)
ANNEX 4: Glasgow commercial building monitoring (*)
ANNEX 5: Air infiltration and ventilation centre
ANNEX 6: Energy systems and design of communities (*)
ANNEX 7: Local government energy planning (*)
ANNEX 8: Inhabitants behaviour with regard to ventilation (*)
ANNEX 9: Minimum ventilation rates (*)
ANNEX 10: Building HVAC system simulation (*)
ANNEX 11: Energy auditing (*)
ANNEX 12: Windows and fenestration (*)
ANNEX 13: Energy management in hospitals (*)
ANNEX 14: Condensation and energy (*)
ANNEX 15: Energy efficiency in schools (*)
ANNEX 16: BEMS 1- User interfaces and system integration (*)
ANNEX 17: BEMS 2- Evaluation and emulation techniques (*)
ANNEX 18: Demand controlled ventilation systems (*)
ANNEX 19: Low slope roof systems (*)
ANNEX 20: Air flow patterns (*)
ANNEX 21: Energy efficient communities (*)
ANNEX 22: Thermal modelling (*)
ANNEX 23: Air flow modelling
ANNEX 24: Heat-Air-Moisture transport in highly insulated envelope parts
ANNEX 25: HEVAC real time simulation and fault detection
ANNEX 26: Air flow in large enclosures
ANNEX 27: Domestic Ventilation Systems
ANNEX 28: Low Energy Cooling
ANNEX 29: Daylighting
ANNEX 30: Bringing simulation models to engineers

ANNEX 24: HEAT-AIR-MOISTURE TRANSPORT IN HIGHLY INSULATED, NEW AND RETROFITTED ENVELOPE PARTS (HAMTIE)

The idea to initiate an Annex on combined heat, air and moisture transport in and through highly insulated envelope parts referred to the fact that, although important, in most countries of the EXCO a methodology to predict and judge the effects of air and moisture flow on instantaneous and average thermal performances, moisture behaviour and durability of envelopes is completely absent. An enquiry in 1989 confirmed this statement. In October 1990, a workshop was organised at the Leuven University, Belgium, focusing on the state of the art in the different countries. This workshop revealed a net need for better basic and applied knowledge of HAM-modelling, environmental conditions and material properties as well as a demand for better use of experimental results. During that meeting, the Annex objectives were formulated as follows:

- to model and study in a fundamental way the physical phenomena of Heat, Air

(*): completed

and Moisture (HAM) transport through new and retrofitted, highly insulated envelope parts;
- to analyse the consequences on the energetical and hygric performances and on the durability of the building envelope.

To reach these objectives, the annex was structured in 5 tasks:

Task 1 *Model and Algorithm development*
This task not only includes improvements in modeling but also testing of simplified models with a potential to predict the combined effects of HAM-transport on thermal quality, hygric behaviour and durability.
Task Leading Country (TLC): Belgium

Task 2 *Indoor and Outdoor Environmental Conditions*
This task includes the choice of environmental parameters, a methodology of handling them and the development of sample sets of environmental conditions.
Task Leading country (TLC): United Kingdom

Task 3 *Material and Layer Properties*
This task includes data collection on thermal, hygric and air properties of materials and layers and substantial measuring work, especially on moisture and air properties.
Task Leading country (TLC): Canada

Task 4 *Experimental verification*
This task includes Hot Box and field tests on HAM-transport in envelope parts, comparison of the measured results with model prediction and transformation of the results into ΔU-rules and durability requirements.
Task Leading country (TLC): Germany

Task 5 *Performances and Practice*
This task includes the translation of HAM-knowledge in performance requirements, correct design and execution of highly insulated new and retrofitted building envelopes.
Task Leading country (TLC): Sweden

Highly insulated was defined by vote as:

$$U \leq 0.30 \text{ W/(m}^2\text{.K)}$$

At first 10, later 14 countries joined together for 4 years of intensified research on HAM:

full BELGIUM, CANADA, DENMARK, FINLAND, FRANCE, GERMANY, ITALY, NORWAY SWEDEN, SWITZERLAND, THE NETHERLANDS, U.K.
observer SLOVAK REPUBLIC, USA

The shared work includes modeling, environmental conditions, material properties, experimental work, common exercises and the draft of interim and final reports. Also the national research efforts are scheduled in accordance with the Annex 24 scheme and the results are brought together and used as base for Annex publications.

Until now, 1 preparation meeting, 1 starting meeting of 3 days, 5 working meetings of 3 days and 2 TLC-meetings were held to build up a common knowledge, to discuss research results and research reports and to elaborate a common performance rationale.

LIST OF EXPERTS CONTRIBUTING TO ANNEX 24

OPERATING AGENT

Belgium
K.U.Leuven, Laboratory of Building Physics,
represented by Prof. H. Hens, head of the laboratory

NATIONAL EXPERTS, FULL MEMBERS

Belgium
National coordinator — A. Janssens (until 28 Feb. 1993)
Mohamed Fatin (since 28 Feb. 1993)
K.U.Leuven, Laboratory of Building Physics
H. Hens, K.U.Leuven, Laboratory of Building Physics
F. Descamps, K.U.Leuven, Laboratory of Building Physics
P. Standaert, Physibel CV

Canada
National coordinator — T. Hamlin (until 23 june 1994)
Duncan Hill (since june 1994)
Canada Mortgage and Housing Corporation
M.K. Kumaran, NRC, IRC, Building Performance Section
A.N. Karagiozis, NRC, IRC, Building Performance Section

Denmark
National coordinator — C.R. Pedersen
Building Research Institute
Prof V. Korsgaard, Technical University of Denmark, Thermal Insulation Lab.

Finland
National coordinator — T. Ojanen
VTT, Technical Research Centre of Finland
M. Salonvaara, VTT, Technical Research Centre of Finland

France

National coordinator — Prof P. Crausse (until 15 Oct. 1992)
Institut de Mechanique des Fluides, Toulouse
B. Perrin (since 15 Oct. 1992)
INSA-UPS, Dept de Genie Civil, Toulouse

T. Duforestel, CSTB
J.F. Daïan, Groupe Hydrology, Grenoble

Germany

National coordinator — K. Kießl
Fraunhofer Institut für Bauphysik, Holzkirchen

H. Künzel, Fraunhofer Institut für Bauphysik, Holzkirchen
M. Krus, Fraunhofer Institut für Bauphysik, Holzkirchen
H. Stopp, Technische Universtät Cottbus, Angewandte Physik
P. Hauppl, Technische Universtät Dresden, Bauklimatik

Italy

National coordinator — C. Lombardi
Politecnico di Torino, Dipartimento del Energetica

Norway

National coordinator — J.V. Thue
Department of Building and Construction
NTH-Trondheim

T. Jacobsen — Building Research Institute, Trondheim

Sweden

National coordinator — C.E. Hagentoft
Department of Building Technology
Chalmers University, Göteborg

J. Arfvidsson, University of Lund, Department of Building Physics
J. Claesson, University of Lund, Department of Building Physics

Switzerland

National coordinator — P. Steiner
EMPA, Sektion Bauphysik

The Netherlands

National coordinator — H. Oldengarm
TNO- Bouw

M. De Wit, Technische Universiteit Eindhoven, Faculteit Bouwkunde, FAGO
Prof. J. Wisse, Technische Universiteit Eindhoven, Faculteit Bouwkunde, FAGO

United Kingdom

National coordinator — C. Sanders
BRE, Scottish Laboratory

P. Burberry, UMIST, Department of Building Engineering
R. Edwards, UMIST, Department of Building Engineering
G. Galbraith, University of Strathclyde, Department of Mechanical Engineering
K. Johnson, Pilkington Insulation Ltd
H. Saidany, University of Bristol

NATIONAL EXPERTS, OBSERVERS

Slovak republic

National coordinator O. Koronthályová
Slovak Academy of Sciences, Institute of Construction and Architecture

P. Matiasovsky, Slovak Academy of Sciences, Institute of Construction and Architecture

USA

National coordinator D.M. Burch
NIST, Gaithersburg

A. Tenwolde, Forest Products Laboratory, Madison

W. Rose, Building Research Council, University of Illinois, Champaign

DESIGN PARAMETERS USED TO AVOID INTERSTITIAL CONDENSATION FOR A RANGE OF CLIMATES

DESIGN PARAMETERS USED TO AVOID INTERSTITIAL CONDENSATION FOR A RANGE OF CLIMATES.

C H Sanders, BRE Scottish Laboratory East Kilbride.

Abstract : This paper summarises the concept of Indoor Climate Classes (ICC) for the assessment of interstitial condensation risk and describes how the 'pivot values' that define the borders between classes can be calculated in worst case constructions with hourly test reference years of climatological data taking radiation into account. The construction and occupancy parameters which affect the ICC are discussed and methods of estimating the pivot values in any 'worst case' construction from monthly mean climate data developed. Data from 93 meteorological stations, ranging from southern Florida to northern Finland and central Canada are analysed to provide the ICC values and limits on moisture production within a house. In many climates surface condensation or mould growth or reverse 'summertime' condensation are likely occur before the onset of interstitial condensation.

1. INTRODUCTION

The risk of moisture damage within building structures, 'interstitial condensation' in its simplest form, is determined by a combination of the structure and the internal and external climates. A more severe external climate will place constraints on the internal climate allowable in any construction before problems start. Further constraints may be placed by the possibility of surface condensation, excessive surface relative humidity and mould growth.

Two approaches to the definition of indoor and outdoor climate are possible. Firstly, statistical data can be collected from as many building types and climates as possible and the appropriate averages, or, for example, the conditions exceeded for 10% of the time, used as driving potentials. Enough hourly meteorological data are available for this to be feasible for external conditions, however, the number of data sets available from within buildings is so small that reliable statistics cannot be estimated for many building types. The alternative approach is to calculate with a more or less sophisticated model the maximum allowable internal vapour pressure before the onset or persistence of interstitial condensation in any construction as a function of external climate and use this as a defining point for internal climate.

This leads to the concept of Indoor Climate Classes (ICC), which has been widely used to define indoor climates in continental Europe, especially Belgium and the Netherlands, for a number of years [1,2]. The boundaries between the classes specify the maximum allowable internal vapour pressure before condensation will occur and persist within certain 'benchmark constructions', which are designed to be 'worst cases' in that they are effectively vapour open to the interior with a perfect vapour seal on the outside. Such constructions are not unrealistic, they are typified by, for example, an unventilated cold deck flat roof, or a wall with metallic cladding.

As the constructions used to define the absolute pivot values are 'worst cases' the resulting climate classes will be conservative in that most real constructions will perform better; the climate class methodology therefore includes a built in safety factor. It is important note two

constraints on this methodology. Firstly, in many climates surface condensation and mould growth will become a problem at internal vapour pressures which are too low to cause interstitial condensation even in the 'worst case' constructions discussed above. Secondly in hot, high radiation climates, reverse or summertime condensation may become a problem, especially in air conditioned buildings as water vapour condenses on a vapour barrier designed to prevent conventional, winter interstitial condensation. Both these factors should be taken into account by designers.

One of the five tasks of IEA Annex 24 is the definition of the internal and external climates relevant to heat, air and moisture transport through building components. It has been decided within Annex 24 to specify three 'pivot points' to define the transitions between the four indoor climate classes: these are :

PIVOT 1 : The maximum monthly mean internal vapour pressure before condensation starts within a north facing wall under mean January conditions

PIVOT 2 : The maximum annual mean internal vapour pressure before there is a net accumulation of condensation over a year within a north facing wall

PIVOT 3 : The maximum annual mean internal vapour pressure before there is a net accumulation of condensation over a year within a flat roof.

To account for the presence of hygroscopic materials, the pivots between classes can be calculated by considering a relative humidity lower than 100% at the inside of the impermeable layer.

An estimate of the pivot values could be made with a simple steady state diffusion calculation (conventionally known as the 'Glaser method' [3]) using monthly mean climate values taking account of radiation with some parameter like the Sol-Air temperature. However, as has been shown[4], this leads to uncertainties in the use of the 'equivalent temperature for condensation' and does not take account of the real radiation climate. To confront these difficulties, 'CLIMCHCK', a simplified version of the full vapour transport model 'MATCH'[5] has been produced within Annex 24[6].

Using the simplified construction represented schematically below, CLIMCHCK uses monthly mean internal conditions and test reference years (TRYs) of hourly external temperature, humidity, solar radiation and wind speed to calculate hourly temperatures at the external surface and the critical layer.

SCHEMATIC DIAGRAM OF CONSTRUCTION ANALYSED BY CLIMCHCK

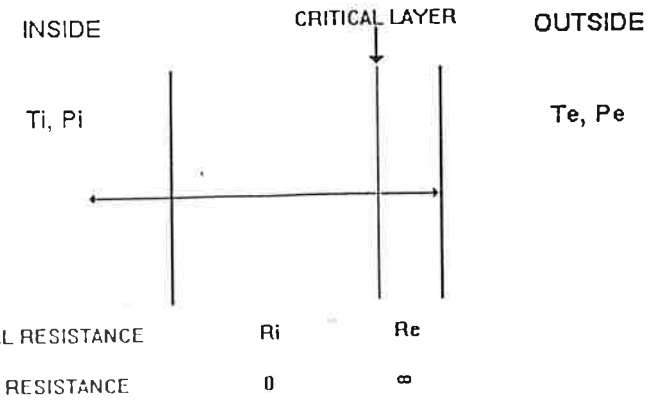

Long wave radiation exchanges are estimated using the humidity data; rainfall is not taken into account as the constructions investigated have an impermeable external layer. The vapour pressure at the critical layer is then calculated from the specified relative humidity. Monthly and annual means which can be used to define the pivot values are stored.

This paper analyses the various factors that affect the pivot values predicted by CLIMCHCK and discusses the values obtained from thirty nine European and fifty one North American climates, ranging from the sub arctic to the sub tropics.

2. THE TEST REFERENCE YEARS AND CONSTRUCTION PARAMETERS USED

The climate data used to calculate the pivot values came from various sources:

a) For Belgium Denmark, France, Eire, Italy, the Netherlands and the UK the EC Test Reference Years (TRYs)[7], were used. These are composite years made up of individual months from different years chosen to give a 'typical' year[8] and contain hourly values of dry bulb temperature, global, direct and diffuse radiation, sunshine duration, relative humidity and wind speed. The quality of the radiation data in these TRYs varies from country to country. Hourly measured values of all three components are available from only three stations (Uccle, Carpentras and Valentia); in most of the other cases, the direct and diffuse components are calculated by unspecified methods from the hourly global component and in some cases all the components are calculated from daily means[7].

The TRYs are all held in the BRE Meteorological Database and were used to calculate the pivot values for France, Eire and Italy and the UK. Papers were received from Belgium[9], the Netherlands[10] and Denmark[11] containing the pivot values calculated for the EC reference years in each country.

b) Papers were received from Germany[12], Slovakia[13], Norway[14] and Finland[15] containing pivot values calculated using test reference years available in each country.

c) Calculations were done for three different locations in Sweden using the Π-factor method[16], which is a variant of the 'CLIMCHCK' method.

d) The ASHRAE Weather Reference Years[17] (WRYs) for 46 locations in the USA and 5 in Canada were received from Doug Burch of NIST. These contain, amongst other data, hourly values of dry bulb, wet bulb and dewpoint temperatures in whole degrees Fahrenheit, windspeeds and a single variable for solar radiation on a horizontal surface. Software developed at NIST[18] was used to calculate the necessary radiation components and the data were converted into the CLIMCHCK input format for calculation of the pivot values.

The location, altitude and relevant climate parameters of the European and North American meteorological stations used are summarised in Tables 1 and 2 respectively, where :

T_{cj} is the January mean dry bulb temperature in °C
P_{cj} is the January mean vapour pressure in Pa
E_{wj} is the January mean global radiation falling on a north facing wall in W/m^2

The location, altitude and relevant climate parameters of the European and North American meteorological stations used are summarised in Tables 1 and 2 respectively, where :

T_{ej} is the January mean dry bulb temperature in °C
P_{ej} is the January mean vapour pressure in Pa
E_{wj} is the January mean global radiation falling on a north facing wall in W/m^2

T_{ey} is the annual mean dry bulb temperature in °C
P_{ey} is the annual mean vapour pressure in Pa
E_{wy} is the annual mean global radiation falling on a north facing wall in W/m^2
E_{ry} is the annual mean global radiation falling on a horizontal surface in W/m^2

As the radiation data from various locations have been derived in different ways it is worth investigating whether there are significant differences between the resultant values calculated by CLIMCHCK from Europe and America. Equations 1, 2 and 3 below are calculated by the regression between E_{wj}, E_{wy} and E_{ry} the cosine of latitude ($\cos\phi$) and the relevant climate parameters.

$$E_{wj} = -49.57 + 114.1\ (\pm 9.1)\cos\phi + 0.42\ (\pm 0.22)\ T_{ej} - 0.014\ (\pm 0.006)\ P_{ej} \quad R^2 = 0.74 \quad (1$$

$$E_{wy} = 7.48 + 81.39\ (\pm 11.2)\cos\phi + 1.29\ (\pm 0.29)\ T_{ey} - 0.022\ (\pm 0.003)\ P_{ey} \quad R^2 = 0.73 \quad (2$$

$$E_{ry} = -35.46 + 295.1\ (\pm 29.3)\cos\phi + 4.02\ (\pm 0.78)\ T_{ey} - 0.065\ (\pm 0.008)\ P_{ey} \quad R^2 = 0.83 \quad (3$$

In these and subsequent regression equations, the standard errors of the coefficients have been included to reflect the range of values and give a measure of the significance of each coefficient.

The means and standard deviations of the residuals from these equations are shown for Europe and America in the table below.

Residuals from :	Europe N=38	America N=51
Ewj	-0.93 ± 5.39	0.69 ± 8.01
Ewy	-0.61 ± 5.39	0.45 ± 6.40
Ery	0.31 ± 17.79	-0.23 ± 14.01

While there are small differences between the mean calculated radiation levels, with the American north wall values being slightly higher than the European ones, these differences are not significant. It can be assumed, therefore, that the methods used to calculate the radiation components give consistent results between the two continents.

To illustrate the range of climates covered, Figures 1 and 2 show the monthly mean temperature, radiation on a horizontal surface and vapour pressure from the hot desert climate of Phoenix, Arizona, the 'sub-tropical' climate of Miami, Florida, the mild 'maritime' climate of Aberporth on the west coast of Wales and the 'Continental' climate of Winnipeg in the prairies of Manitoba.

FIGURE 1 :MONTHLY MEAN RADIATION AGAINST TEMPERATURE FOR FOUR STATIONS

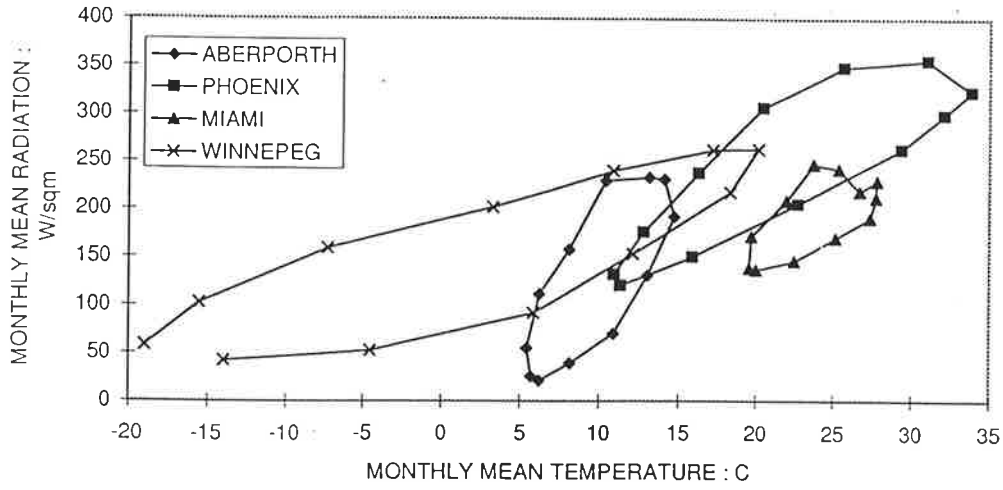

FIGURE 2 :MONTHLY MEAN VAPOUR PRESSURE AGAINST TEMPERATURE FOR FOUR STATIONS

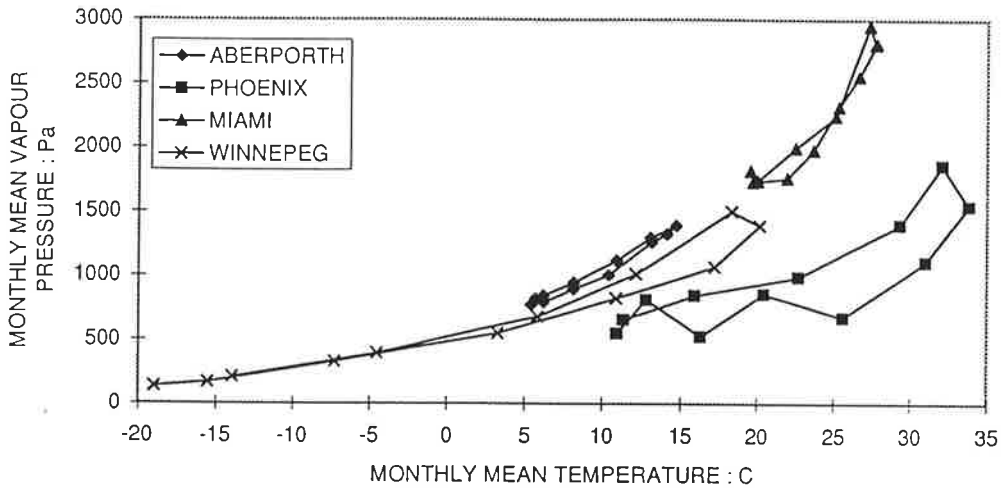

Besides the hourly climate data input from the TRY, the calculated pivot values are also affected by construction and occupancy parameters. The most important of these, with the values taken as standard by Annex 24, are :

T_{ij} : the mean inside temperature during January = 21°C
T_{iy} : the mean inside temperature over the year = 21°C

R_i : the R value between the critical layer and the inside air = 3.0 m^2K/W
R_o : the R value between the critical layer and the outside surface = 0.1 m^2K/W

(note : the outside surface resistance is calculated hour by hour from the radiation parameters and the wind speed in the TRY)

3. FACTORS AFFECTING THE PIVOT VALUES DERIVED BY CLIMCHCK

The pivot values calculated with CLIMCHCK are based on the climate of the specific locations and the standard values of the various input parameters for the construction. To calculate precise values for any other location and other 'worst case' construction types a test reference year of hourly climatic data is needed to run CLIMCHCK. As this is not generally available for many locations, regression equations have been developed between the three pivot values and a) the values of R_i and R_e, b) the internal temperature and c) the solar absorptivity. The coefficients of these equations, whose format is summarised in the table below, are themselves linear functions of the climate means and can therefore be used to estimate values for any construction type in any location for which monthly mean climatic data are available.

INPUT PARAMETERS	PIVOT 1	PIVOT 2	PIVOT 3
R_e/R_i	B_{11}	B_{12}	B_{13}
INTERNAL TEMPERATURE	B_{21}	B_{22}	B_{23}
SOLAR ABSORBTIVITY	B_{31}	B_{31}	B_{33}

To linearise the various factors in terms of a simple, easily accessible climate parameter, the critical layer mean temperatures in January and over the year were calculated from :

$$T_{cj} = T_{ej} + (T_{ij} - T_{ej}) \times \frac{(R_e + R_{so})}{(R_e + R_i + R_{so})} \quad (4$$

$$T_{cy} = T_{ey} + (T_{iy} - T_{ey}) \times \frac{(R_e + R_{so})}{(R_e + R_i + R_{so})} \quad (5$$

Where R_i and R_e are as defined above, R_{so} is the conventionally defined external surface resistance (taken as 0.04 m^2K/W in all cases) and the temperature subscripts are :

j : January mean	c : calculated
y : annual mean	e : exterior
	i : interior

T_{cj} and T_{cy} are therefore the simply defined critical layer mean temperatures, taking no account of radiation, equivalent temperature for condensation etc. The saturated vapour pressures at T_{cj} and T_{cy}, $P_s(T_{cj})$ (for pivot 1) and $P_s(T_{cy})$ (for pivots 2 and 3) have been used to establish linear relationships with the pivot values.

a) Inside and outside thermal resistances

Figure 3 shows the values of pivot 1 in Pa calculated for Winnipeg using the standard parameters, but with a range of values of R_i and R_e, plotted against $P_s(T_{cj})$ and Figure 4 the pivot 3 values from Trapani against $P_s(T_{cy})$.

FIGURE 3: WINNIPEG PIVOT 1 VALUES AGAINST FOR DIFFERENT COMBINATIONS OF Re/Ri

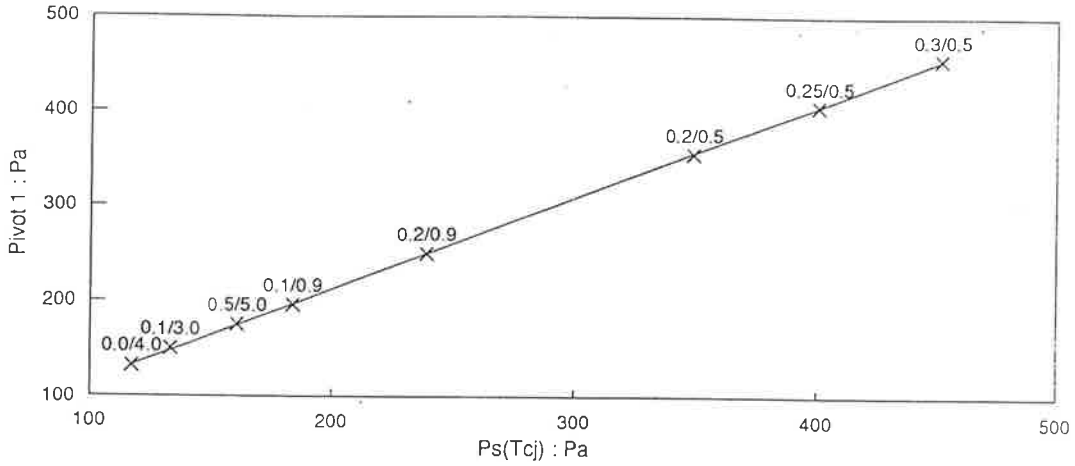

FIGURE 4: TRAPANI PIVOT 3 VALUES AGAINST Ps(Tcy) FOR DIFFERENT COMBINATIONS OF Re/Ri

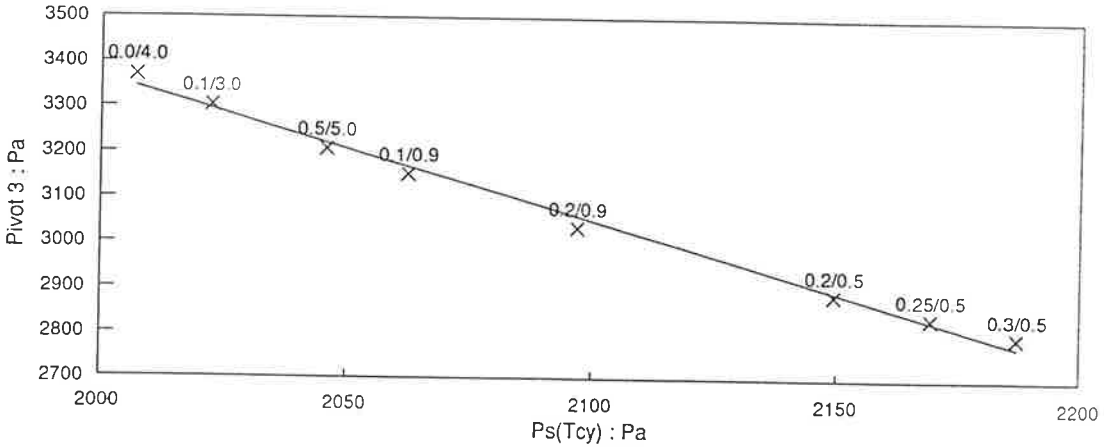

The regression equations for the three pivot values from Winnipeg and Trapani are:

Winnipeg
$P1 = 19.52 + 0.964\ (\pm 0.003)\ P_s(T_{cj})$ $R^2 = 0.9998$
$P2 = 597.4 + 0.637\ (\pm 0.005)\ P_s(T_{cy})$ $R^2 = 0.9994$ (6
$P3 = 1406.9 + 0.351\ (\pm 0.016)\ P_s(T_{cy})$ $R^2 = 0.9860$

Trapani
$P1 = -91.4 + 1.032\ (\pm 0.005)\ P_s(T_{cj})$ $R^2 = 0.9998$
$P2 = 952.5 + 0.581\ (\pm 0.009)\ P_s(T_{cy})$ $R^2 = 0.9973$ (7
$P3 = 9836.6 - 3.230\ (\pm 0.084)\ P_s(T_{cy})$ $R^2 = 0.9932$

Where P1, P2 and P3 are the pivot points in Pascals

The three values from all the stations give similar linear relationships of the form :

$$\text{Pivot 1} = A_{11} + B_{11}\, P_s(T_{cj})$$
$$\text{Pivot 2} = A_{21} + B_{21}\, P_s(T_{cy})$$
$$\text{Pivot 3} = A_{31} + B_{31}\, P_s(T_{cy})$$

To investigate the effect of climate on the coefficients, B_{11}, B_{21} and B_{31} the pivot values were calculated for all the stations for which TRYs were available using the standard values of T_i and solar absorptivity a, but with $R_i = 0.5$ and $R_e = 0.3$. B_{11} was then calculated from

$$B_{11} = \frac{Pl_{(0.1\,/\,3.0)} - Pl_{(0.3\,/\,0.5)}}{P_s(T_{cj})_{(0.1\,/\,3.0)} - P_s(T_{cj})_{(0.3\,/\,0.5)}} \qquad (8$$

with similar equations for B_{21} and B_{31}. The resulting coefficients are shown in Tables 3 and 4.

FIGURE 5 : B31 AGAINST ANNUAL MEAN TEMPERATURE

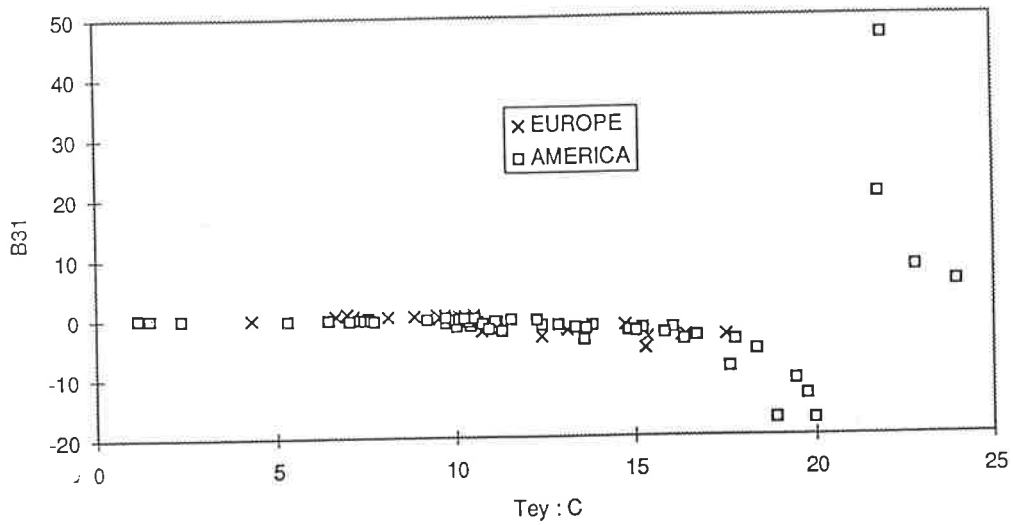

The pattern of the data in Figure 5, which shows the variation of B_{31} with outside annual mean temperature, is due to the changing importance of radiative gains from the outside and conductive heat transfer from the inside to the critical plane as the outside temperature changes. In all climates where the outside mean conditions are cooler than inside, if the relative values of R_e and R_i are changed so that the ratio $R_e/(R_e+R_i)$ rises, the critical plane will tend to become warmer due to conduction from the inside but tend to become cooler as the effect of radiative gain on the outside surface is less. In a cold, low radiation external climate the net effect will be warming, as shown in Figure 3. In hot, high radiation environment the net effect will be cooling, as shown in Figure 4. In the limit, at an external temperature of 21°C, equal to the internal temperature, the change in critical layer temperature calculated by CLIMCHCK as $R_e/(R_e+R_i)$ is changed will be entirely due to the radiation on the outside surface and, as the values of T_{cj} and T_{cy}, calculated by equations 4 and 5, will be constant, the coefficients B_{11}, B_{21}

and B_{31} will go to $-\infty$. If , as in the case of four of the stations in the southern USA, the external annual mean temperature is higher than 21°C, the conductive and radiative effects will combine as $R_e/(R_e+R_i)$ is changed, giving the large positive coefficients shown in Figure 5.

It is important to note that, in high temperature, high radiation environments, reverse or 'summertime' interstitial condensation may be a significant problem, especially in air conditioned buildings. Water vapour driven in by the high external temperatures can condense on a vapour check positioned to eliminate the risk of conventional or 'winter' condensation. This possibility should be allowed for in the design of structures in these climates.

FIGURE 6: B31 AGAINST CORRECTED ANNUAL MEAN TEMPERATURE

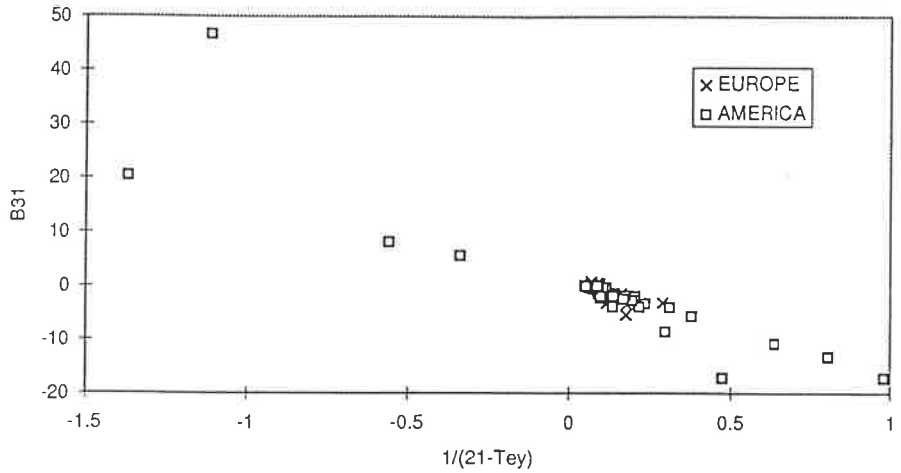

As shown Figure 6, this effect can be linearised by plotting B_{31} against $1/(21 - T_{ey})$; the one obvious outlier is from Phoenix, Arizona, a desert environment with exceptionally high radiation levels. The three coefficients can then be well predicted from the environmental data with following regression equations.

$$B_{11} = 1.410 - 0.511(\pm 0.048)\ TR._j - 0.00054(\pm 0.00036)\ E_{wj} - 0.061(\pm .0087)\ C \quad R^2 = 0.762 \quad (9$$

$$B_{21} = 1.83 - 2.497(\pm 0.094)\ TR._y - 0.0095(\pm 0.0028)\ E_{wy} - 0.255(\pm 0.055)\ C \quad R^2 = 0.913 \quad (10$$

$$B_{31} = 5.25 - 16.317(\pm 0.536)\ TR._y - 0.033\ (\pm 0.0044)\ E_{ry} + 0.363\ (\pm 0.308)\ C \quad R^2 = 0.933 \quad (11$$

Where : $TR_j = 1/(21 - T_{ej})$
$TR_y = 1/(21 - T_{ey})$
C = 1 for Europe and 2 for America

Despite the apparent consistency between the two sets of radiation data discussed above, there is a significant difference between the B_{11} and B_{21} values in Europe and America.

b) Internal Temperature

If the three pivot values are calculated for internal temperatures varying from 15 to 25°C and correlated with $P_s(T_{cj})$ and $P_s(T_{cy})$ respectively, exact linear relationships result in each case. The coefficients B_{12}, B_{22} and B_{32} from the stations with TRYs are shown in Tables 3 and 4, which shows that there is relatively little variation between stations. This is confirmed by the equations resulting from correlation of the three coefficients with the relevant external temperatures and radiation intensities shown below.

$$B_{12} = 0.987 - 0.0039(\pm 0.0011)\, T_{cj} + 0.0032(\pm 0.0008)\, E_{wj} - 0.0251(\pm 0.0195)C \quad R^2 = 0.243 \quad (12$$

$$B_{22} = 1.011 - 0.0097(\pm 0.0021)\, T_{cy} + 0.0033(\pm 0.0012)\, E_{wy} + 0.0268(\pm 0.0208)C \quad R^2 = 0.228 \quad (13$$

$$B_{32} = 0.975 - 0.0303(\pm 0.0066)\, T_{cy} - 0.0074(\pm 0.0010)\, E_{ry} - 0.1175(\pm 0.058)\, C \quad R^2 = 0.428 \quad (14$$

Using these equations to derive the coefficients is only slightly better than taking an overall average value for all stations.

c) Solar absorptance of external surface.

Figure 7 shows the variation of the three pivot values with the solar absorptance of the external surface calculated with the standard values of the other parameters.

FIGURE 7 : PIVOT VALUES FROM ABERPORTH AND TRAPANI AS A FUNCTION OF SOLAR ABSORPTANCE

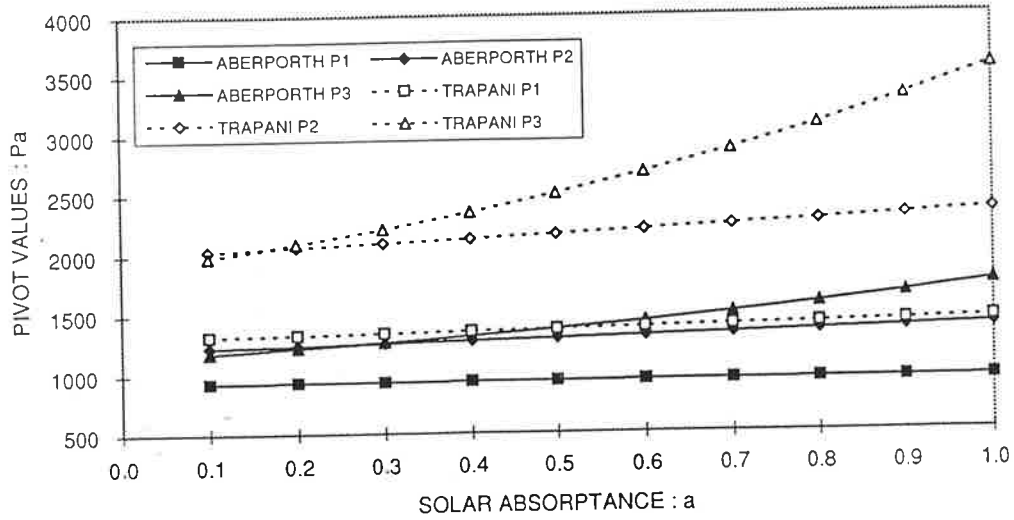

The pivot values can be represented to a very high degree of precision ($R^2 > .9999$) by equations of the form

$$Pn = A + B_1 \times a + B_2 \times a^2 + B_3 \times a^3$$

However, the error in assuming linear relationships is very small for practical purposes. The coefficients for P1, P2 and P3, B_{13}, B_{23} and B_{33} respectively, are summarised in Tables 3 and 4 and the regression equations for their prediction from the relevant outside temperature and radiation intensity are :

$$B_{13} = -30.28 + 3.506\ (\pm 0.734)\ T_{cj} + 6.304\ (\pm 0.494)\ E_{wj} - 35.55(\pm 12.57)\ C \quad R^2 = 0.823 \quad (15$$

$$B_{23} = -610.6 + 6.97\ (\pm 3.27)\ T_{cy} + 17.14\ (\pm 1.75)\ E_{wy} - 50.27(\pm 31.44)\ C \quad R^2 = 0.709 \quad (16$$

$$B_{33} = -1255.7 + 36.49\ (\pm 14.91)\ T_{cy} + 18.94\ (\pm 2.25)\ E_{ry} - 404.7(\pm 130.1)\ C \quad R^2 = 0.690 \quad (17$$

d) The relative importance of the three parameters

The relative importance of the three parameter corrections developed above can be assessed from the absolute percentage change, averaged over all stations, in the pivot values when the parameters undergo the maximum likely change, shown in the table below :

PARAMETER CHANGE	% CHANGE IN PIVOT 1	% CHANGE IN PIVOT 2	% CHANGE IN PIVOT 3
THERMAL RESISTANCE R_e/R_i: 0.1/3.0 to 0.3/0.5	62.6	14.7	13.5
TEMPERATURE T_i: 15°C to 25°C	3.2	2.9	2.6
SOLAR ABSORPTIVITY a : 0.1 to 1.0	9.6	21.5	50.0

As might be expected, the value of pivot 1, which is little affected by radiation, is strongly dependant on the value of R_e/R_i , while Pivot 3 depends strongly on the solar absorptivity. Internal temperature is much less important than the other two parameters.

4. EFFECT OF DIFFERENT CLIMATES

The three pivot values calculated using the standard parameters from all the stations are shown in Tables 5 and 6.

Figures 8, 9 and 10 show the three pivot values plotted against $P_s(T_{cj})$ and $P_e(T_{cy})$ for all the stations, with Europe and America distinguished. The values from the three Swedish stations, calculated with the Π-factor method, have also been shown separately on these figures; it can be seen that they are consistent with the remaining values calculated with CLIMCHCK.

FIGURE 8 : PIVOT 1 AGAINST Ps(Tcj)

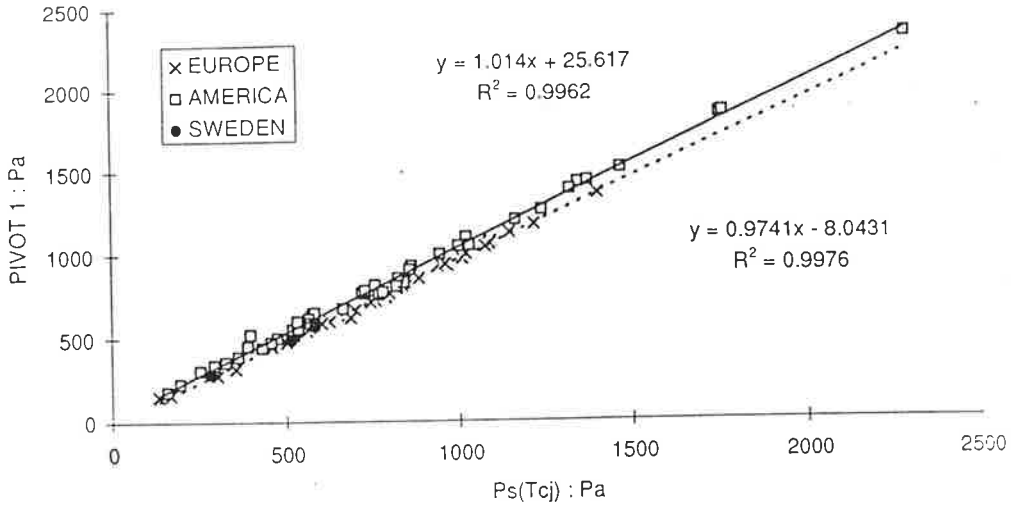

FIGURE 9 : PIVOT 2 AGAINST Ps(Tcy)

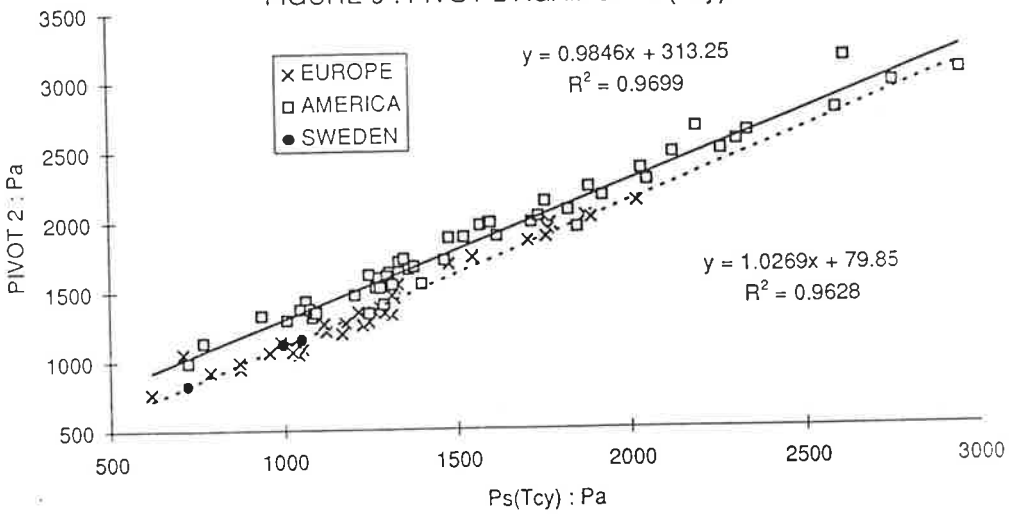

FIGURE 10 : PIVOT 3 AGAINST Ps(Tcy)

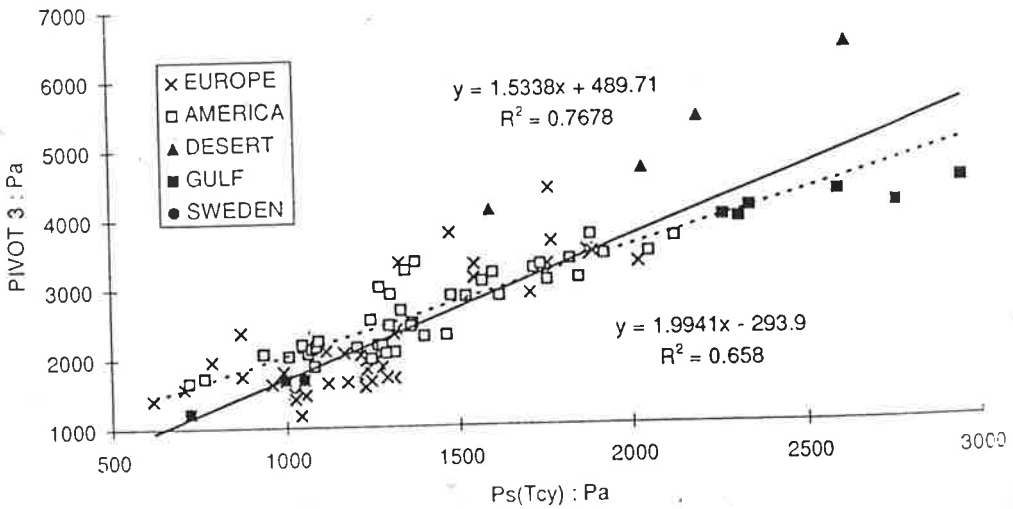

The calculated regression equations between the pivot values and the climate parameters are :

$$P1 = -78.75 + 0.985\ (\pm.007)\ P_s(T_{cj}) + 1.111\ (\pm0.256)\ E_{wj} + 44.77(\pm6.26)\ C \quad R^2 = 0.997 \quad (18$$

$$P2 = -185.0 + 0.945\ (\pm.019)\ P_s(T_{cy}) + 4.640\ (\pm0.944)\ E_{wy} + 131.8(\pm18.5)\ C \quad R^2 = 0.981 \quad (19$$

$$P3 = -749.2 + 1.114\ (\pm.115)\ Ps(T_{cy}) + 13.61\ (\pm1.628)\ E_{ry} - 206.1(\pm97.4)\ C \quad R^2 = 0.863 \quad (20$$

As noted in section 3a), significant differences between the continents remain for all the pivot values after external temperature and radiation have been taken into account. It is possible that this is due to differences in the way the climate reference years, especially the radiation data, have been constructed in the two continents. It may, however, reflect a real climatic difference between the European stations, which are mainly in climate zones influenced by the sea, and the American stations, many of which have a generally continental climate. No systematic difference emerges if the stations are split overall into 'coastal' and 'continental' groups. However, as shown on Figure 10, there is a systematic difference between the stations around the Gulf of Mexico, which are hot and humid, and those in the desert areas of Texas, New Mexico, Arizona and Nevada which are hot and dry with very high radiation levels.

5. ESTIMATION OF PIVOT VALUES FROM MONTHLY MEAN DATA

As the test reference year of hourly climatic data needed to run CLIMCHCK is not generally available for many locations, the regression equations developed in sections 3 and 4 above can be used to estimate values for any construction type in any location for which monthly mean climatic data are available.

For simplicity, the procedure is outlined below for estimation of the first pivot value alone. parallel steps can be followed to estimate the second and third pivots.

a) Equation 18 is used to calculate the standard pivot value from the January mean external temperature and north wall radiation and the continent.

b) To allow for a non-standard value of R_i or R_e, equation 9 is used to calculate B_{11} and equation 4 used to calculate T_{cj}. An inverted form of equation 8 is then used to calculate the pivot value.

$$P1_{(ns)} = P1_{(s)} - B_{11}\ (Ps(Tcj)_{(s)} - Ps(Tcj)_{(ns)}) \quad (21$$

Where the subscript 's' refers to the standard values and 'ns' to the non standard values of R_i and R_e.

c) To allow for a non standard internal temperature, equation 12 is used to calculate B_{12} and equation 4 used to calculate T_{cj}. Equation 22 is then used to calculate the pivot value.

$$P1_{(ns)} = P1_{(s)} - B_{12}\ (Ps(Tcj)_{(s)} - Ps(Tcj)_{(ns)}) \quad (22$$

Where the subscripts 's' and 'ns' refer to the standard and non standard temperatures.

d) To allow for a non standard solar absorptance, equation 15 is used to calculate B_{13} and the pivot value calculated from :

$$P1_{(ns)} = P1_{(s)} - B_{13}(a_{s,s} - a_{(ns)}) \qquad (23$$

Where the subscripts 's' and 'ns' refer to the standard and non standard absorptivities.

6. EFFECTIVE PIVOT VALUES

Tables 5 and 6 show the relative humidities that result from the calculated pivot vapour pressures at the assumed internal temperature of 21°C. Many of the vapour pressures given as pivots 2 and 3 in the warmer climates are higher than the saturation vapour pressure at 21°C. In those cases 100% RH is reported in the tables. Also, many of the pivot 2 values are over 70% leading to the internal surface relative humidities over 80% which cause surface mould growth before interstitial condensation becomes a problem.

The coefficients B_{12}, B_{22} and B_{32} in Tables 3 and 4 can be used to calculate the pivot value vapour pressures as a function of internal temperature. The internal surface temperatures can then be calculated from :

$$Tsi = Ti - (Ti - Te)\frac{Rsi}{Rso + Re + Ri' + Rsi} \qquad (24$$

Where Tsi is the internal surface temperature in °C
Rsi is the internal surface resistance in m^2K/W
$Ri' = Ri - Rsi$ in m^2K/W
and the remaining symbols are as defined in section 3.

The internal surface relative humidity at each of the pivot points can then be calculated from

$$RHin = 100\frac{Pn}{Ps(Tsi)} \qquad (25$$

Where Pn is the vapour pressure at the nth pivot point in Pa
Ps(Tsi) is the saturated vapour pressure at Tsi in Pa
Rhin is the internal surface relative humidity at the nth pivot point in %.

Figure 11 shows, for Aberporth and Trapani, the internal surface relative humidity at the pivot points against internal temperature calculated with Rsi = 0.125 m^2K/W. Pivot 3 at Trapani leads to surface relative humidities always above 80%, the accepted limit for mould growth[19], when the temperature is lower than 30°C, suggesting that surface mould growth will be a problem before interstitial condensation in this climate, whatever the roof design or internal humidity conditions, provided that the internal temperature is below 30°C. In contrast, at Aberporth, with much lower radiation levels, the comparable limit temperature is 18°C. As 'worst case' constructions are modelled by CLIMCHCK, these will be conservative limits. However, as shown in the work of IEA Annex XIV, 'Condensation and Energy'[19], the value of Rsi = 0.125 m^2K/W taken in Figure 11 is a minimum; values as high as 0.5 m^2K/W may occur in

corners, behind furniture etc. These will lead to slightly lower surface temperatures and consequently higher internal surface relative humidities.

FIGURE 11 : INTERNAL SURFACE RELATIVE HUMIDITY AT PIVOT POINTS AGAINST INTERNAL AIR TEMPERATURE

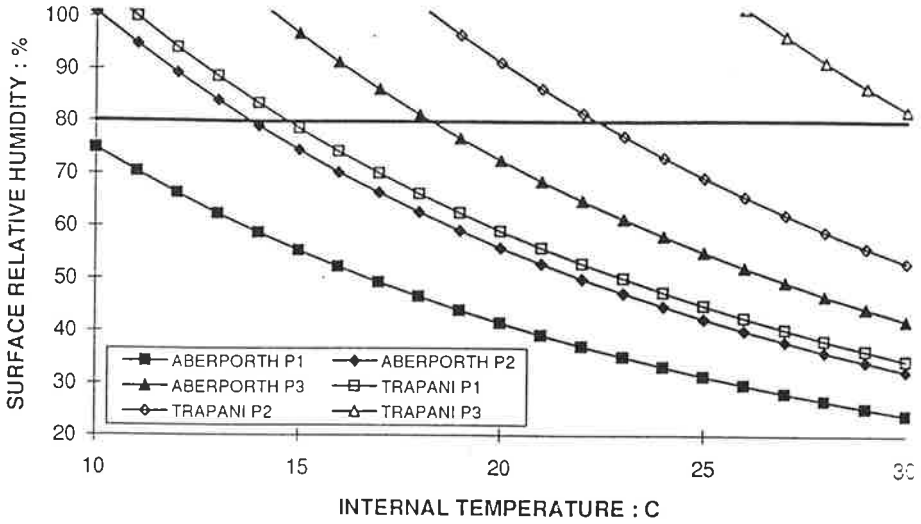

7. ALLOWABLE MOISTURE GENERATION RATES

The difference between the pivot values in Tables 5 and 6 and the outside vapour pressures in Tables 1 and 2 can be converted into an excess moisture content for each station, $\rho i - \rho e$ g/m³. By assuming a building volume and ventilation these can be converted to the maximum moisture generation rate that keeps the internal conditions below the pivot value.

$$G = nV(\rho i - \rho e) \times 24 / 1000 \quad \text{kg/day} \qquad (26$$

Where n is the ventilation rate and V the volume of the house. Taking n= 0.5 ach and V= 250m³ and constraining the internal surface relative humidity below 80% to avoid mould growth (using the methodology of equations 24) and 25)) gives the values of G shown in Tables 5 and 6. These are plotted against the mean external vapour pressure on Figures 12, 13 and 14. Figure 13 and especially Figure 14 show that for most of the American stations and many European the need to keep internal surface relative humidities below 80% to avoid surface mould growth is a more important constraint on moisture production than the risk of interstitial condensation. In two of the stations around the Gulf of Mexico the external annual mean vapour pressure exceeds the internal value that would lead to 80% at the inside surface. In the absence of air conditioning the internal temperatures in this region would be considerably higher than 21°C, however in practice the internal air is both cooled and dried, eliminating the risk of surface mould or conventional interstitial condensation but bringing a real risk of reverse or 'summertime' condensation as water diffuses into the building.

FIGURE 12 :ALLOWABLE MOISTURE RELEASE TO KEEP BELOW P1 OR PREVENT SURFACE MOULD GROWTH AGAINST OUTSIDE VAPOUR PRESSURE

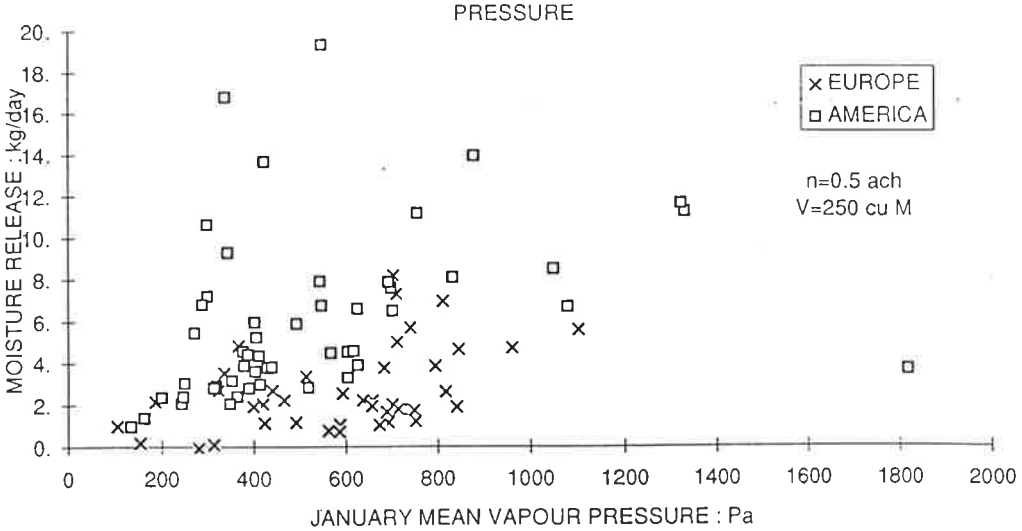

FIGURE 13 :ALLOWABLE MOISTURE RELEASE TO KEEP BELOW P2 OR PREVENT SURFACE MOULD GROWTH AGAINST OUTSIDE VAPOUR PRESSURE

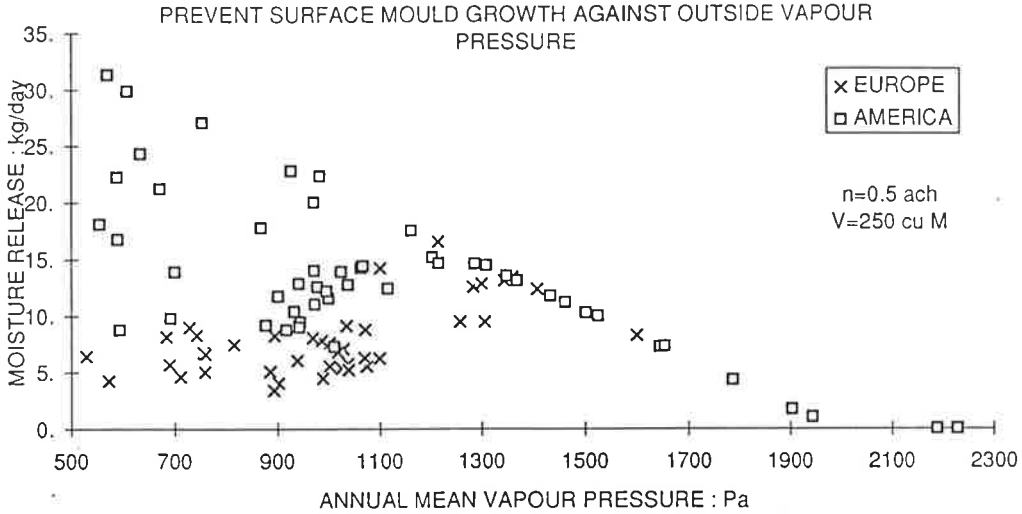

FIGURE 14 :ALLOWABLE MOISTURE RELEASE TO KEEP BELOW P3 OR PREVENT SURFACE MOULD GROWTH AGAINST OUTSIDE VAPOUR PRESSURE

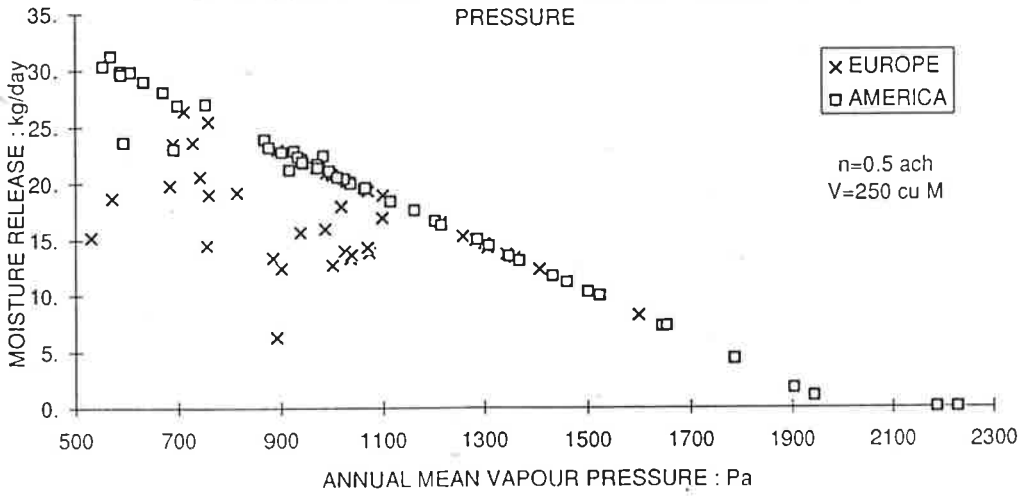

8. GEOGRAPHICAL DISTRIBUTION OF PIVOT VALUES

Figures 15, 16 and 17 show the locations of the stations and contours of the three pivot values from Table 5 for Europe. Figures 18, 19 and 20 show the contours of the allowable moisture release, constrained below an internal surface relative humidity of 80%, for the three pivots. Figures 21 to 26 show the same information for America.

a) Europe

As the Pivot 1 value is dominated by the January external temperature, it is not surprising that Figure 15 shows a distinct trend from the cold north east in Finland to the warmer Mediterranean climates. Pivot 3 is much more strongly affected by radiation and so Figure 17 shows a distinct minimum around the mild humid North Atlantic and a pronounced maximum around southern Italy; a less pronounced maximum is also visible around the south of Finland, which will be influenced by the high summer radiation levels in the Siberian Anticyclone.

This pattern is emphasised in Figures 19 and 20 which show that, if the values are constrained below a surface relative humidity of 80%, the influence of both the Atlantic and the Mediterranean limit the moisture production within houses much more than in the centre of the continent.

b) America

Figures 21 to 23 show that all the pivots increase from with increasing temperature from north to south. The high radiation environments of the deserts in the south west of the USA show much higher pivot 3 values than the more humid, but similarly warm areas around the Gulf of Mexico.

Figures 25 and 26 emphasise that the warm humid conditions around the Gulf of Mexico limit moisture production severely in non air conditioned buildings. While in the centre of the continent much higher production levels are possible.

9. CONCLUSIONS

This paper summarised the concept of Indoor Climate Classes (ICC) for the assessment of interstitial condensation risk described how the 'pivot values' that define the borders between classes can be calculated in worst case constructions with hourly test reference years of climatological data taking radiation into account. The construction and occupancy parameters which affect the ICC were used to develop methods of estimating the pivot values in any 'worst case' construction from monthly mean climate data. Data from 93 meteorological stations, ranging from southern Florida to northern Finland and central Canada were analysed to provide the ICC values and limits on moisture production within a house. In many climates surface condensation leading to mould growth or reverse 'summertime' condensation are likely occur before the onset of interstitial condensation and should be taken into account by designers working in these areas.

10. REFERENCES

1. Van der Kooy J. 1973, De temperatuur en vochtigheid in woningen, Klimaatbeheersing, 1973 nr 10, pp490-496.

2. Vos B.H. & Tammes E. 1974, Kursus Warmteisolatie , opleidingen Bouwcentrum, IBBC-TNO, 1974.

3. Glaser H., 1958, Vereinfachte Berechnung der Dampfdiffusion durch geschichtete Wande bei Ausscheidung von Wasser und Eis. Kaltetechnik, Band 10 (1958), pp 358 - 364.

4. Hens 1992 . Indoor Climate Classes IEA Annex 24 paper T2 - B 92/02.

5. Pedersen 1992, Prediction of Moisture Transfer in Building Constructions, Building and Environment, Vol 27, No 3, pp 387-397, 1992.

6. Rode 1993 , Determination of simplified indoor/outdoor climate conditions for HAMTIE Calculations, the CLIMCHCK program. IEA Annex 24 paper T2-DK-93/01 .

7. CEC 1985, Test Reference Years TRY : Commission of the European Communities Directorate General XII fir Science, Research and Development, 1985

8. EUR 1977 Selection Methods for the Production of Test Reference Years. Hans Lund, Stig Eidorff. Final Report of contract 284-77 ES DK. Report EUR 7306 EN.

9. Reports on the Environmental Conditions for HAMTIE : F. Ali Mohamed : T2-B-94/01

10. Indoor Climate Classes : Pivot values for three TRY locations in the Netherlands Hans Oldengarm T2-NL-94/02

11. Pivot Values for Internal Climate Classes, Denmark. C. Rode: T2-DK-93/03

12. Reports on the Environmental Conditions in Germany, H. Fechner and J. Grunewald : T2-D-94/01

13. Indoor Climate Classes for Slovakia, O.Koronthalyova and P. Matiasovsky : T2-SK-94/03.

14. Norwegian Indoor Climate Classes calculated by the CLIMCHCK Program. S. Geving : T2-N-94/01

15. Determination of indoor climate classes for Finland. Ojanen, & Salonvaara T2-SF-93/01

16. Presentation of Pivot Values Calculated by the Π-factor Method for Three Different Locations in Sweden ; E. Harderup : T2-S-94/02.

17: Weather Year for Energy Calculations : L. W. Crow : ASHRAE Journal June 1984.

18. Fortran program - Solar.for : Doug Burch NIST 1994.

19. IEA Annex XIV 'Condensation and Energy', Sourcebook March 1991.

TABLES AND CONTOUR MAPS

TABLE 1 : Summary of European Stations and Climate Data

COUNTRY	STATION	LAT N	LONG	ALT m	Tej °C	Pej Pa	Ewj W/m²	Tey °C	Pey Pa	Ewy W/m²	Ery W/m²
BELGIUM	SAINT-HUBERT	50°02'	05°24'E	563	-2.2	492	19.9	6.7	885	50.5	109.3
	UCCLE	50°48'	04°21'E	105	3.7	748	14.8	10.1	1099	50.1	107.6
	OOSTENDE	51°12'	02°52'E	4	3.6	753	14.9	9.5	1038	56.2	123.4
DENMARK	COPENHAGEN	55°46'	12°19'E	19	-0.6	563	7.5	8.1	939	43.5	116.2
FRANCE	NICE	43°39'	07°12'E	10	7.7	703	17.8	14.7	1283	61.4	168.8
	CARPENTERAS	44°05'	05°03'E	105	5.5	711	30.0	13.1	1100	67.1	177.0
	LIMOGES	45°49'	01°17'E	284	3.3	701	23.2	10.6	1035	58.7	147.4
	MACON	46°18'	04°48'E	217	2.7	658	18.8	10.5	1071	57.9	140.9
	NANCY	48°41'	06°13'E	204	2.9	687	15.1	9.5	1003	55.3	125.9
	TRAPPES	48°46'	02°01'E	168	3.4	720	16.9	9.9	1030	53.4	124.7
IRELAND	VALENTIA	51°56'	10°15'W	20	6.5	796	13.6	10.5	1074	50.6	119.1
	DUBLIN	53°26'	06°15'W	85	5.8	841	9.1	9.5	1003	45.2	117.9
ITALY	TRAPANI	37°55'	12°30'E	14	11.6	1103	27.7	17.5	1599	62.1	207.8
	CROTONE	39°04'	17°04'E	158	8.4	812	28.8	16.3	1360	60.1	188.6
	CAGLIARI	39°15'	09°03'E	18	9.4	962	26.3	16.4	1409	59.7	199.7
	FOGGIA	41°31'	15°43'E	56	6.6	741	26.3	15.4	1216	59.2	183.2
	ROMA	41°48'	12°35'E	161	7.6	846	25.6	15.3	1344	58.8	187.9
	MONTE TERMINILLO	42°28'	12°59'E	1875	-3.5	337	23.7	4.3	691	48.2	143.3
	GENOVA	44°25'	08°51'E	3	7.4	711	22.2	15.2	1300	54.8	161.3
	MILANO	45°26'	09°17'E	103	0.6	587	21.3	12.4	1258	54.0	144.6
	VENEZIA	45°30'	12°20'E	6	2.6	637	22.5	13.1	1307	53.8	162.5
	BOLZANO	46°28'	11°20'E	241	-1.1	368	26.1	10.7	996	54.6	147.8
HOLLAND	VLISSINGEN	51°27'	03°36'E	22	3.3	713	15.5	10.3	1071	51.8	115.2
	DE BILT	52°06'	05°11'E	40	2.5	656	14.7	9.5	1020	51.4	112.4
	EELDE	53°08'	06°35'E	5	2.7	692	11.8	8.8	1027	51.8	111.9
U K	KEW (LONDON)	51°28'	00°19'W	77	4.4	683	13.4	10.3	988	45.1	106.9
	ABERPORTH	52°08'	04°34'W	133	5.7	818	13.1	9.7	1040	51.0	125.4
	ESKDALEMUIR	55°19'	03°12'W	242	2.2	672	8.1	7.1	902	41.8	94.2
	LERWICK	60°08'	01°11'W	82	2.9	689	6.1	7.0	893	40.0	88.6
FINLAND	HELSINKI	60°10'	24°57'E	46	-8.5	314	4.5	4.3	760	36.2	105.2
	JYVASKYLA	62°18'	26°08'E	55	-10.6	281	3.6	2.8	712	36.0	94.4
	SODANKYLA	67°40'	26°39'E	180	-18.3	154	0.7	-0.8	573	36.8	85.4
NORWAY	OSLO	59°55'	10°44'E	94	-3.8	423	5.9	6.2	730	40.8	110.6
	BERGEN	60°24'	5°19'E	43	1.0	514	5.7	6.7	757	36.2	88.6
GERMANY	ESSEN	51°24'	6°59'E	154	1.9	595	14	9.5	969	49.4	112.1
	MUNCHEN	48°08'	11°43'E	530	-3.2	420	20.9	8.0	894	49.2	122.4
	BREMERHAVEN	55°31'	8°35'E	7	0.7	587	10.6	8.7	990	25.6	79.6
SLOVAKIA	BRATISLAVA	48°10'	17°08'E	153	-2.0	440	13.0	9.3	941	39.4	133.2
	POPRAD	49°03'	20°12'E	800	-5.0	325	13.0	5.7	761	41.3	139.3
SWEDEN	SÄVE	57°42'	11°58'E	41	-1.6	465	10.4	7.1	817	58.4	108.6
	BROMMA	59°21'	18°04'E	44	-3.4	400	8.4	6.3	744	55.6	109.2
	LULEA	65°33'	22°08'E	10	-11.5	188	1.6	1.5	531	47.0	95.9

TABLE 2 : Summary of North American Stations and Climate data

STATION	LAT N	LONG W	ALT m	Tej °C	Pej Pa	Ewj W/m^2	Tey °C	Pey Pa	Ewy W/m^2	Ery W/m^2
BIRMINGHAM, AL	33.5	86.8	186	6.3	699	34.3	16.7	1462	57.7	174.2
PHOENIX , AZ	33.5	112	340	11.0	550	60.5	21.9	985	88.7	243.7
LITTLE ROCK, AR	34.7	92.2	78	4.1	626	32.8	16.4	1502	62.6	183.3
LOS ANGELES, CA	34.0	118.2	60	12.3	879	64.7	16.1	1287	84.9	209.9
DENVER, CO	39.8	104.8	1610	-1.9	301	43.4	10.0	590	69.9	204.7
WASHINGTON, DC	38.8	77.0	5	1.6	493	26.6	13.9	1204	55.4	157.7
MIAMI, FL	25.8	80.3	3	19.6	1818	47.2	24.0	2230	66.2	192.6
TALLAHASSEE, FL	30.3	84.3	18	11.3	1050	42.7	19.4	1787	65.2	186.2
TAMPA, FL	28.0	82.5	6	15.2	1331	46.4	21.7	1945	67.4	194.5
ATLANTA, GA	33.7	84.5	306	5.5	702	34.9	15.8	1434	59.3	175.1
BOISE, ID	43.5	116.2	866	-1.8	406	31.5	10.4	672	77.2	194.2
CHICAGO, IL	41.9	87.8	190	-3.2	391	24.0	10.4	973	54.5	168.6
INDIANOPOLIS, IN	39.7	86.3	242	-3.3	414	24.5	11.2	1115	56.0	151.4
DES MOINES, IA	41.5	93.7	289	-7.2	321	27.1	9.7	1038	60.7	171.0
DODGE CITY, KS	37.8	100.0	791	-2.1	430	39.1	12.4	973	68.9	203.1
LAKE CHARLES, LA	30.2	93.2	4	10.7	1080	40.8	19.8	1904	67.6	177.4
PORTLAND, ME	43.7	70.3	19	-5.8	315	22.2	7.6	917	52.7	136.7
BOSTON, MA	42.3	71.0	5	-1.7	378	23.6	10.5	978	54.1	143.3
DETROIT, MI	42.3	83.0	193	-4.5	355	23.0	9.2	973	53.7	146.0
MINNEAPOLIS, MN	44.8	93.1	251	-11.0	245	23.4	7.3	902	56.7	152.3
KANAS CITY, MO	39.2	94.7	226	-2.1	413	30.6	13.4	1163	63.0	174.9
ST LOUIS, MO	38.7	90.3	150	-1.7	520	31.0	12.9	1216	62.2	173.0
GREAT FALLS, MT	47.5	111.3	1117	-7.0	273	28.1	7.0	555	67.1	164.5
OMAHA, NB	41.3	95.8	298	-5.1	365	29.7	10.8	1063	60.4	172.4
LAS VEGAS, NV	36.2	115.2	659	6.7	339	53.7	18.9	570	82.3	242.8
ALBEQUERQUE, NM	35.0	106.7	1618	1.4	344	62.6	13.6	609	87.3	237.4
NEW YORK CITY, NY	40.8	73.8	10	0.3	403	26.8	12.3	1067	56.4	142.1
RALEIGH, NC	35.8	78.5	132	4.0	545	33.7	14.8	1349	59.5	168.6
BISMARK, ND	46.8	100.8	502	-13.0	202	22.3	5.3	700	62.3	163.8
CLEVELAND, OH	41.3	81.8	237	-2.9	404	22.8	10.0	1001	53.0	142.5
DAYTON, OH	39.8	84.2	304	-2.1	440	25.7	11.1	1026	55.0	151.2
OKLAHOMA CITY, OK	35.3	97.7	390	2.2	606	40.1	15.2	1309	69.0	190.3
MEDFORD, OR	42.3	122.8	396	2.4	606	32.8	11.3	870	74.4	177.6
PORTLAND, OR	45.6	122.7	10	3.7	618	23.4	11.6	997	61.7	139.4
PITTSBURG, PA	40.5	80.0	228	-2.8	381	23.4	10.1	942	54.7	139.4
CHARLESTON, SC	32.8	80.0	10	8.7	834	32.0	17.8	1644	58.9	175.6
NASHVILLE, TN	36.2	86.7	176	3.4	548	26.6	15.1	1369	54.1	164.4
AMARILLO, TX	35.1	101.7	1099	1.6	300	57.3	13.7	927	80.3	216.6
BROWNSVILLE, TX	25.8	97.5	5	15.3	1322	51.4	22.8	2189	75.0	201.3
DALLAS, TX	32.8	96.8	147	6.8	693	41.5	18.4	1525	68.9	192.0
EL PASO, TX	31.8	106.3	1194	6.3	424	47.7	17.6	755	74.1	248.3
SAN ANTONIO, TX	29.5	98.3	241	9.7	757	42.6	20.0	1653	68.1	195.5
SALT LAKE CITY, UT	40.8	112	1286	-1.9	389	39.9	10.9	634	75.5	209.4
SEATTLE, WA	47.5	122.3	20	3.3	628	19.7	10.2	933	61.2	137.0
MADISON, WI	43.2	89.3	262	-8.2	251	24.7	7.4	944	55.0	155.1
CHEYENNE, WY	41.2	104.7	1621	-2.9	290	39.0	7.6	590	66.8	193.8
EDMONTON, Canada	53.6	113.5	206	-16.3	165	16.0	1.5	595	58.1	142.5
MONTREAL, Canada	45.5	73.7	10	-9.6	248	20.8	6.5	878	50.2	143.6
TORONTO, Canada	43.7	79.6	54	-5.9	350	23.0	7.7	943	53.3	154.3
VANCOUVER, Canada	49.2	123.2	2	2.6	569	19.8	9.7	1012	60.0	137.3
WINNEPEG, Canada	49.9	97.2	73	-19.0	135	18.6	2.4	693	54.9	154.1

TABLE 3 : Coefficients for Correction of Pivot Values to Standard Parameters (Europe)

COUNTRY	STATION	B11	B21	B31	B12	B22	B32	B13	B23	B33
BELGIUM	SAINT-HUBERT	0.983	0.873	0.471	0.964	1.065	1.334	34.3	223.4	642.9
	UCCLE	0.982	0.835	0.205	0.985	1.072	1.348	38.1	282.0	813.7
	OOSTENDE	0.987	0.879	0.494	0.940	0.972	1.175	38.2	202.7	576.0
DENMARK	COPENHAGEN	0.989	0.862	0.363	0.949	1.061	1.340	14.0	188.4	707.7
FRANCE	NICE	0.977	0.680	-1.332	0.943	1.067	1.519	112.0	483.9	1621.0
	CARPENTERAS	1.000	0.646	-1.755	1.114	1.200	1.854	179.4	570.6	2125.1
	LIMOGES	0.997	0.804	-0.516	0.992	1.144	1.672	62.7	412.0	1483.6
	MACON	1.007	0.765	-0.440	1.046	1.160	1.638	54.3	410.0	1370.3
	NANCY	1.004	0.830	0.014	0.994	1.134	1.508	38.1	344.3	1041.1
	TRAPPES	0.991	0.864	0.053	0.989	1.116	1.488	42.5	324.1	1029.9
IRELAND	VALENTIA	0.998	0.956	0.513	0.931	0.989	1.208	28.2	185.3	636.8
	DUBLIN	1.000	0.935	0.579	0.956	0.995	1.193	22.3	164.9	559.1
ITALY	TRAPANI	1.034	0.597	-3.084	1.027	1.036	1.459	132.7	349.5	1758.6
	CROTONE	0.989	0.546	-3.286	0.993	1.123	1.688	95.7	440.5	2205.6
	CAGLIARI	1.035	0.646	-3.121	1.084	1.074	1.650	133.8	377.7	2163.3
	FOGGIA	1.000	0.498	-3.347	1.059	1.149	1.846	108.8	472.9	2496.0
	ROMA	1.023	0.598	-5.288	1.104	1.250	2.315	129.2	588.7	3672.3
	MONTE TERMINILLO	0.986	0.903	-0.013	1.005	1.080	1.779	54.9	185.1	1223.4
	GENOVA	0.999	0.695	-2.500	0.999	1.114	1.728	81.5	418.4	2159.8
	MILANO	1.062	0.652	-3.152	1.212	1.365	2.444	90.0	623.0	3194.9
	VENEZIA	1.051	0.658	-2.161	1.175	1.236	2.004	102.7	474.7	2397.6
	BOLZANO	1.043	0.693	-2.178	1.258	1.367	2.430	132.1	567.1	2798.1
HOLLAND	VLISSINGEN	0.979	0.885	0.439	0.920	0.991	1.199	31.6	204.2	620.7
	DE BILT	0.995	0.856	0.224	0.967	1.107	1.407	38.1	293.8	856.6
	EELDE	1.010	0.862	0.400	0.989	1.060	1.300	29.3	238.8	674.4
U K	KEW (LONDON)	0.987	0.902	0.449	0.935	1.043	1.256	28.9	207.2	646.0
	ABERPORTH	0.972	0.931	0.494	0.877	0.965	1.198	22.3	183.2	630.5
	ESKDALEMUIR	1.006	0.957	0.529	0.974	1.114	1.398	19.4	214.5	678.4
	LERWICK	0.985	0.961	0.845	0.902	0.944	1.037	10.8	103.9	269.4

TABLE 4 : Coefficients for Correction of Pivot Values to Standard Parameters (America)

STATION	B11	B21	B31	B12	B22	B32	B13	B23	B33
BIRMINGHAM, AL	0.932	0.247	-3.256	1.070	1.146	1.623	126.2	421.1	1930.9
PHOENIX , AZ	0.868	7.529	46.632	1.127	1.202	2.097	513.9	1551.8	5028.1
LITTLE ROCK, AR	0.899	0.012	-3.922	1.031	1.167	1.717	79.8	517.6	2215.5
LOS ANGELES, CA	0.928	0.762	-1.888	1.054	1.057	1.521	429.1	555.4	1814.2
DENVER, CO	0.946	0.525	-1.470	1.129	1.193	1.984	146.4	537.3	2149.1
WASHINGTON, DC	0.933	0.444	-1.318	1.013	1.130	1.551	56.1	354.6	1484.2
MIAMI, FL	0.620	1.364	5.490	1.008	1.030	1.377	268.0	513.1	2114.3
TALLAHASSEE, FL	0.886	-0.717	-10.636	1.095	1.115	1.591	215.3	541.7	2227.5
TAMPA, FL	0.766	3.649	20.406	1.053	1.047	1.410	244.5	503.1	1969.5
ATLANTA, GA	0.917	0.367	-2.711	1.069	1.119	1.636	124.4	430.5	1957.1
BOISE, ID	0.929	0.506	-1.333	1.105	1.206	1.898	77.6	663.5	1995.7
CHICAGO, IL	0.972	0.527	-0.628	0.966	1.161	1.611	34.7	302.4	1291.2
INDIANOPOLIS, IN	0.941	0.504	-0.664	1.009	1.162	1.577	41.4	337.1	1254.8
DES MOINES, IA	0.937	0.470	-0.797	1.123	1.195	1.708	42.9	387.4	1416.4
DODGE CITY, KS	0.933	0.300	-1.269	0.982	1.117	1.567	69.3	395.6	1491.0
LAKE CHARLES, LA	0.880	-1.375	-13.178	1.035	1.095	1.523	173.3	561.9	2090.7
PORTLAND, ME	0.964	0.700	0.047	0.998	1.154	1.516	27.9	269.8	898.3
BOSTON, MA	0.954	0.635	-0.047	0.948	1.076	1.356	34.2	258.8	847.4
DETROIT, MI	0.942	0.620	-0.223	0.975	1.154	1.542	25.9	278.6	1047.3
MINNEAPOLIS, MN	0.959	0.532	-0.204	1.135	1.226	1.624	29.1	304.5	989.5
KANAS CITY, MO	0.931	0.254	-1.677	1.040	1.177	1.666	57.5	469.0	1685.9
ST LOUIS, MO	0.920	0.354	-1.247	1.087	1.156	1.597	71.4	417.6	1491.4
GREAT FALLS, MT	0.881	0.594	-0.404	1.129	1.189	1.723	37.7	481.8	1293.4
OMAHA, NB	0.964	0.422	-0.973	1.024	1.204	1.700	43.8	394.6	1473.2
LAS VEGAS, NV	0.893	-1.736	-17.163	1.095	1.158	2.073	365.4	1024.4	4157.8
ALBEQUERQUE, NM	0.961	0.250	-3.786	1.120	1.202	2.144	346.1	962.0	3236.6
NEW YORK CITY, NY	0.947	0.554	-0.333	0.914	1.081	1.367	36.7	300.6	958.2
RALEIGH, NC	0.920	0.399	-2.243	1.027	1.167	1.701	97.3	456.1	1924.0
BISMARK, ND	0.938	0.537	-0.303	1.120	1.282	1.806	19.4	364.1	1141.3
CLEVELAND, OH	0.936	0.613	-0.255	0.995	1.131	1.491	31.2	265.5	1028.1
DAYTON, OH	0.929	0.533	-0.584	1.024	1.144	1.546	43.3	312.0	1213.5
OKLAHOMA CITY, OK	0.915	0.123	-1.827	1.002	1.085	1.451	90.0	425.7	1431.7
MEDFORD, OR	1.019	0.544	-2.204	1.145	1.276	2.140	161.1	918.7	2664.7
PORTLAND, OR	0.991	0.759	-0.320	1.055	1.109	1.498	81.8	443.5	1221.0
PITTSBURG, PA	0.951	0.632	-0.222	1.008	1.159	1.508	36.6	294.9	1035.1
CHARLESTON, SC	0.924	0.109	-3.965	1.044	1.094	1.505	129.2	414.3	1787.9
NASHVILLE, TN	0.936	0.332	-2.417	1.002	1.151	1.679	66.4	404.6	1921.8
AMARILLO, TX	0.921	0.260	-1.896	1.011	1.117	1.636	163.9	570.8	1842.8
BROWNSVILLE, TX	0.766	2.144	8.042	0.989	1.005	1.301	232.3	490.5	1761.4
DALLAS, TX	0.949	-0.608	-5.652	0.975	1.065	1.459	123.7	510.4	1824.6
EL PASO, TX	0.921	-0.259	-8.490	1.020	1.123	1.926	184.5	696.1	3427.3
SAN ANTONIO, TX	0.945	-2.203	-17.225	1.038	1.078	1.526	177.1	543.7	2209.8
SALT LAKE CITY, UT	0.974	0.398	-1.902	1.055	1.209	1.986	125.4	687.2	2316.4
SEATTLE, WA	0.981	0.825	-0.039	0.982	1.070	1.443	56.6	398.5	1077.0
MADISON, WI	0.958	0.621	-0.271	1.053	1.217	1.695	31.5	283.3	1147.9
CHEYENNE, WY	0.914	0.653	-0.302	1.017	1.117	1.627	70.7	342.6	1239.9
EDMONTON, Canada	0.974	0.729	0.020	1.136	1.328	1.993	13.9	388.3	1076.1
MONTREAL, Canada	0.959	0.655	-0.196	1.065	1.232	1.741	23.7	268.7	1124.1
TORONTO, Canada	0.968	0.667	-0.458	1.042	1.215	1.793	39.3	310.5	1369.1
VANCOUVER, Canada	0.979	0.867	0.068	0.994	1.106	1.486	59.1	394.0	1056.1
WINNEPEG, Canada	0.961	0.611	-0.013	1.064	1.326	1.859	9.8	267.5	935.7

TABLE 5 : Summary of Calculated Pivot Values and Allowable Moisture Generation Rates for Europe

COUNTRY	STATION	P1 Pa	P2 Pa	P3 Pa	RH1 %	RH2 %	RH3 %	G1 kg/day	G2 kg/day	G3 kg/day
BELGIUM	SAINT-HUBERT	544	1113	1489	22	45	60	1.2	5.1	13.4
	UCCLE	826	1378	1858	33	55	75	1.7	6.2	16.9
	OOSTENDE	806	1297	1639	32	52	66	1.2	5.8	13.3
DENMARK	COPENHAGEN	597	1211	1641	24	49	66	0.8	6.1	15.6
FRANCE	NICE	1071	1850	2893	43	74	100	8.2	12.6	15.0
	CARPENTERAS	936	1739	3109	38	70	100	5.0	14.2	18.9
	LIMOGES	791	1445	2382	32	58	96	2.0	9.1	20.1
	MACON	758	1467	2323	30	59	93	2.2	8.8	19.3
	NANCY	759	1347	1972	31	54	79	1.6	7.6	20.7
	TRAPPES	800	1347	1966	32	54	79	1.8	7.0	20.1
IRELAND	VALENTIA	969	1323	1698	39	53	68	3.9	5.5	13.9
	DUBLIN	927	1252	1577	37	50	63	1.9	5.5	12.8
ITALY	TRAPANI	1355	2128	3305	55	86	100	5.6	8.3	8.3
	CROTONE	1124	2027	3486	45	82	100	6.9	13.5	13.5
	CAGLIARI	1174	2011	3468	47	81	100	4.7	12.4	12.4
	FOGGIA	997	1974	3633	40	79	100	5.7	16.6	16.6
	ROMA	1056	1935	4396	42	78	100	4.7	13.1	13.7
	MONTE TERMINILLO	497	947	1751	20	38	70	3.6	5.7	23.5
	GENOVA	1039	1879	3300	42	76	100	7.3	12.9	14.7
	MILANO	634	1687	3772	26	68	100	1.0	9.5	15.3
	VENEZIA	737	1734	3305	30	70	100	2.2	9.5	14.3
	BOLZANO	586	1546	3357	24	62	100	4.8	12.2	21.0
HOLLAND	VLISSINGEN	794	1352	1716	32	54	69	1.8	6.2	14.3
	DE BILT	743	1326	1827	30	53	73	1.9	6.8	17.9
	EELDE	744	1267	1658	30	51	67	1.2	5.3	14.0
U K	KEW (LONDON)	853	1340	1705	34	54	69	3.8	7.8	15.9
	ABERPORTH	936	1275	1657	38	51	67	2.6	5.2	13.7
	ESKDALEMUIR	718	1083	1463	29	44	59	1.0	4.0	12.5
	LERWICK	764	1046	1179	31	42	47	1.7	3.4	6.3
FINLAND	HELSINKI	319	988	2371	13	40	95	0.1	5.1	25.5
	JYVASKYLA	278	921	1959	11	37	79	0.0	4.6	26.4
	SODANKYLA	162	766	1415	7	31	57	0.2	4.3	18.7
NORWAY	OSLO	474	1136	1793	19	46	72	1.1	9.0	23.6
	BERGEN	666	1062	1410	27	43	57	3.4	6.8	14.5
GERMANY	ESSEN	709	1331	1951	29	54	78	2.5	8.0	21.4
	MUNCHEN	513	1264	2088	21	51	84	2.1	8.2	22.9
	BREMERHAVEN	619	1191	2061	25	48	83	0.7	4.5	20.9
SLOVAKIA	BRATISLAVA	562	1349	2029	23	54	82	2.7	9.1	22.0
	POPRAD	447	1060	1618	18	43	65	2.7	6.6	19.0
SWEDEN	SÄVE	565	1152	1682	23	46	68	2.2	7.5	19.2
	BROMMA	486	1118	1671	20	45	67	1.9	8.3	20.6
	LULEÄ	285	822	1214	11	33	49	2.1	6.5	15.2

TABLE 6 : Summary of Calculated Pivot Values and Allowable Moisture Generation Rates for America

STATION	P1 Pa	P2 Pa	P3 Pa	RH1 %	RH2 %	RH3 %	G1 kg/day	G2 kg/day	G3 kg/day
BIRMINGHAM, AL	1039	2168	3430	42	87	100	7.6	11.2	11.2
PHOENIX , AZ	1422	3148	6425	57	100	100	19.4	22.4	22.4
LITTLE ROCK, AR	923	2232	3706	37	90	100	6.6	10.3	10.3
LOS ANGELES, CA	1506	1945	3106	61	78	100	13.9	14.6	15.1
DENVER, CO	625	1590	3001	25	64	100	7.2	22.2	29.9
WASHINGTON, DC	758	1887	2847	31	76	100	5.9	15.2	16.7
MIAMI, FL	2317	3059	4449	93	100	100	3.6	0.0	0.0
TALLAHASSEE, FL	1432	2493	3958	58	100	100	8.5	4.3	4.3
TAMPA, FL	1838	2773	4068	74	100	100	11.3	1.0	1.0
ATLANTA, GA	994	2067	3361	40	83	100	6.5	11.8	11.8
BOISE, ID	643	1628	2901	26	65	100	5.3	21.2	28.1
CHICAGO, IL	518	1603	2446	21	64	98	2.8	14.0	21.4
INDIANOPOLIS, IN	549	1673	2478	22	67	100	3.0	12.4	18.4
DES MOINES, IA	452	1611	2536	18	65	109	2.9	12.7	19.9
DODGE CITY, KS	601	1875	2863	24	75	100	3.8	20.0	21.7
LAKE CHARLES, LA	1382	2564	3926	56	100	100	6.7	1.7	1.7
PORTLAND, ME	442	1309	1868	18	53	75	2.8	8.7	21.1
BOSTON, MA	584	1542	2068	23	62	83	4.6	12.5	21.3
DETROIT, MI	497	1469	2135	20	59	86	3.2	11.0	21.3
MINNEAPOLIS, MN	338	1429	2055	14	57	83	2.1	11.7	22.7
KANAS CITY, MO	610	1962	3057	25	79	100	4.4	17.5	17.5
ST LOUIS, MO	647	1876	2844	26	75	100	2.8	14.7	16.3
GREAT FALLS, MT	519	1368	2178	21	55	88	5.5	18.1	30.4
OMAHA, NB	474	1702	2660	19	68	100	2.4	14.2	19.5
LAS VEGAS, NV	1095	2663	5396	44	100	100	16.8	31.3	31.3
ALBEQUERQUE, NM	762	1978	4086	31	80	100	9.3	29.9	29.9
NEW YORK CITY, NY	671	1714	2306	27	69	93	6.0	14.4	19.5
RALEIGH, NC	901	1982	3237	36	80	100	7.9	13.6	13.6
BISMARK, ND	306	1324	2050	12	53	82	2.3	13.9	27.0
CLEVELAND, OH	567	1520	2175	23	61	88	3.6	11.5	20.8
DAYTON, OH	611	1650	2427	25	66	98	3.8	13.9	20.3
OKLAHOMA CITY, OK	810	2131	3067	33	86	100	4.5	14.5	14.5
MEDFORD, OR	754	1670	3357	30	67	100	3.3	17.8	23.8
PORTLAND, OR	825	1544	2286	33	62	92	4.6	12.2	21.0
PITTSBURG, PA	556	1518	2157	22	61	87	3.9	12.8	22.1
CHARLESTON, SC	1197	2278	3453	48	92	100	8.1	7.3	7.3
NASHVILLE, TN	851	2023	3293	34	81	100	6.7	13.1	13.1
AMARILLO, TX	778	1978	3181	31	80	100	10.6	22.8	22.8
BROWNSVILLE, TX	1847	2964	4123	74	100	100	11.6	0.0	0.0
DALLAS, TX	1046	2475	3675	42	100	100	7.8	10.0	10.0
EL PASO, TX	1039	2362	4659	42	95	100	13.7	27.0	27.0
SAN ANTONIO, TX	1259	2624	4087	51	100	100	11.1	7.3	7.3
SALT LAKE CITY, UT	588	1726	3238	24	69	100	4.4	24.3	29.0
SEATTLE, WA	803	1399	2054	32	56	83	3.9	10.3	22.3
MADISON, WI	388	1369	2111	16	55	85	3.0	9.4	21.8
CHEYENNE, WY	595	1342	2150	24	54	87	6.8	16.7	29.6
EDMONTON, Canada	226	990	1659	9	40	67	1.4	8.8	23.6
MONTREAL, Canada	356	1289	2010	14	52	81	2.4	9.1	23.1
TORONTO, Canada	443	1345	2235	18	54	90	2.1	8.9	21.8
VANCOUVER, Canada	770	1337	1972	31	54	79	4.5	7.2	20.5
WINNEPEG, Canada	179	1132	1730	7	46	70	1.0	9.8	23.0

FIGURE 15 Contours of Pivot 1 for Europe

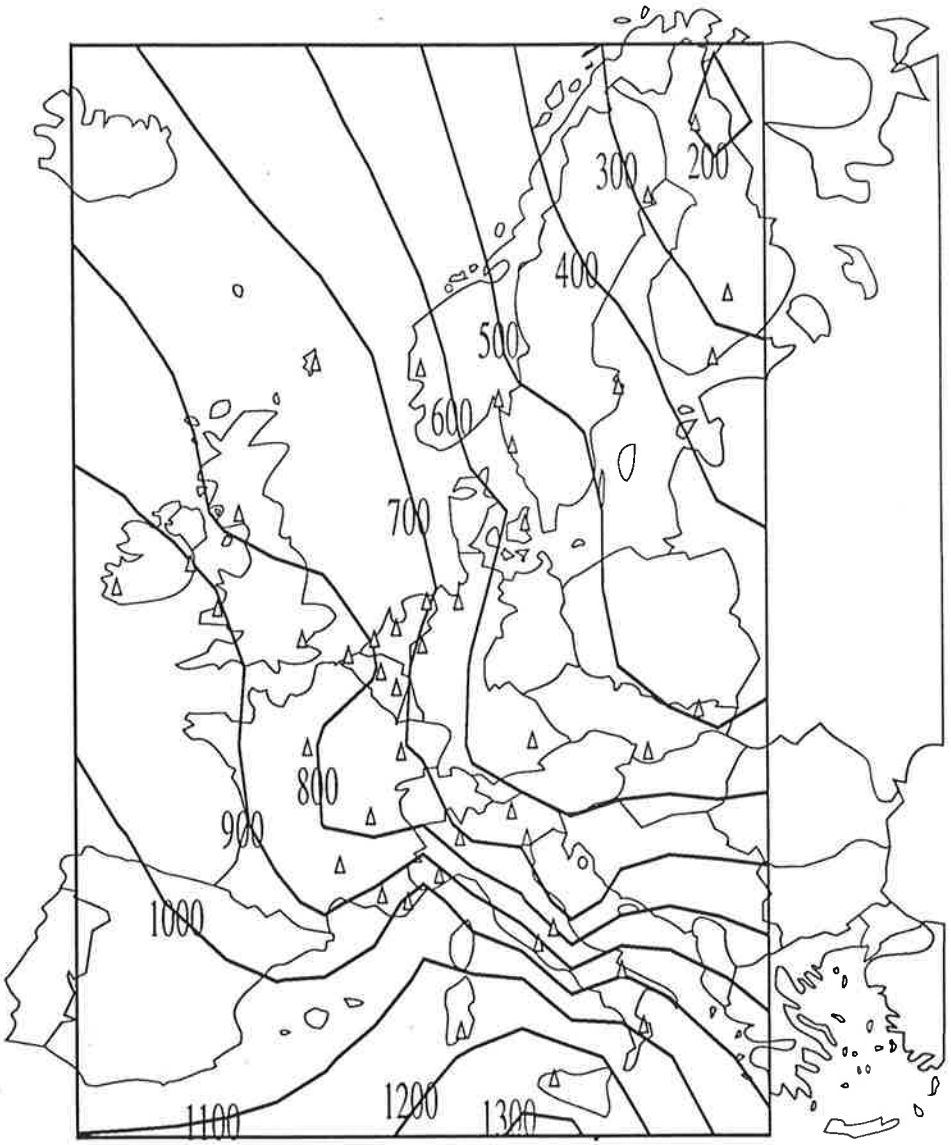

FIGURE 16 Contours of Pivot 2 for Europe

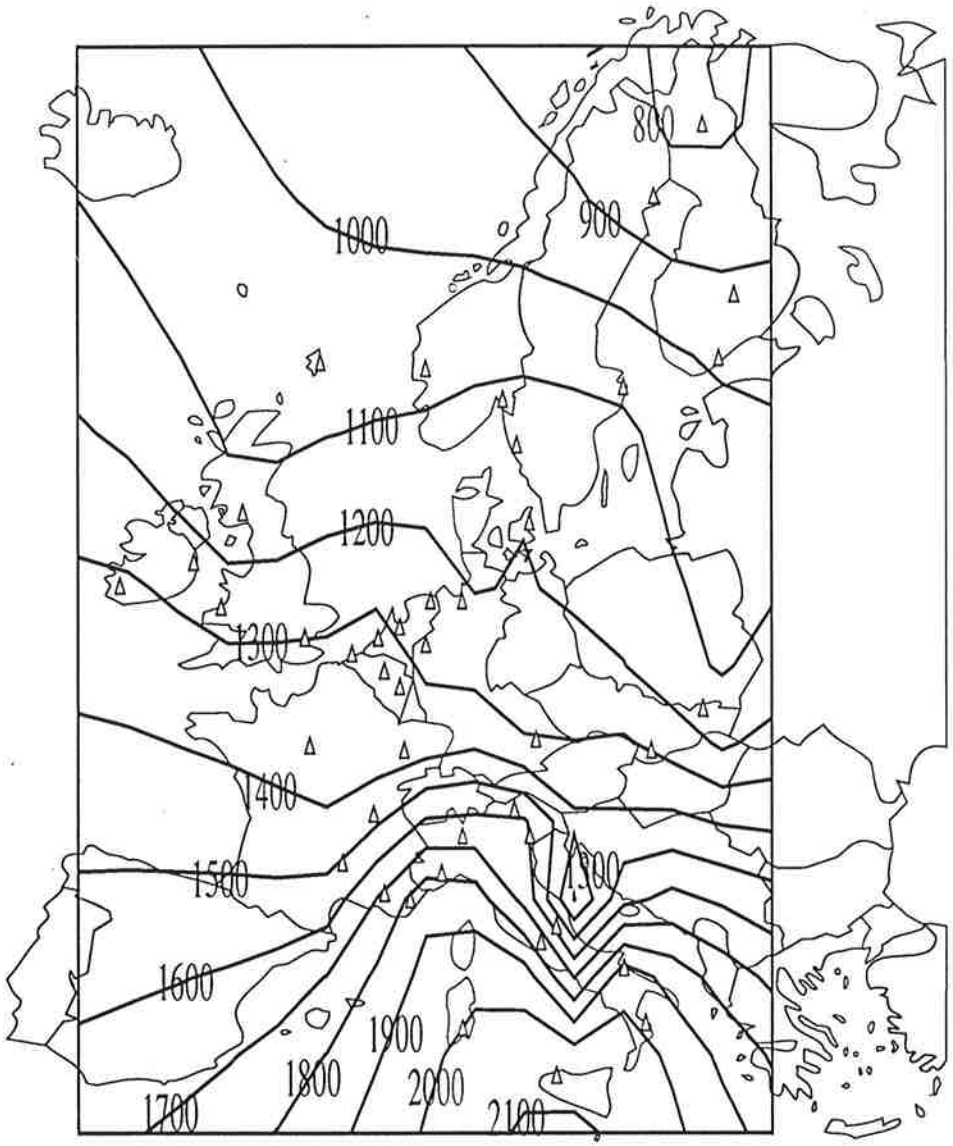

FIGURE 17 Contours of Pivot 3 for Europe

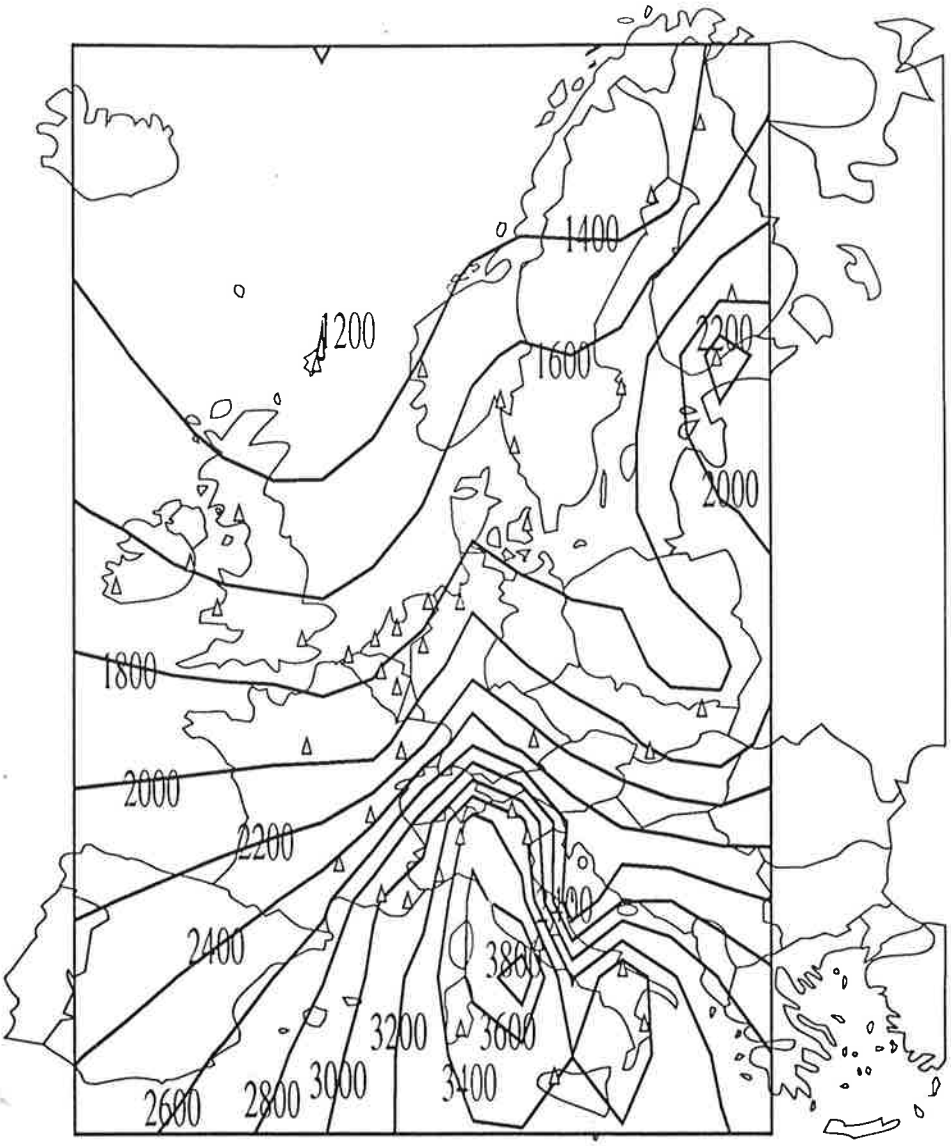

FIGURE 18 Contours of Allowable Moisture Release for the P1 Pivot in Europe

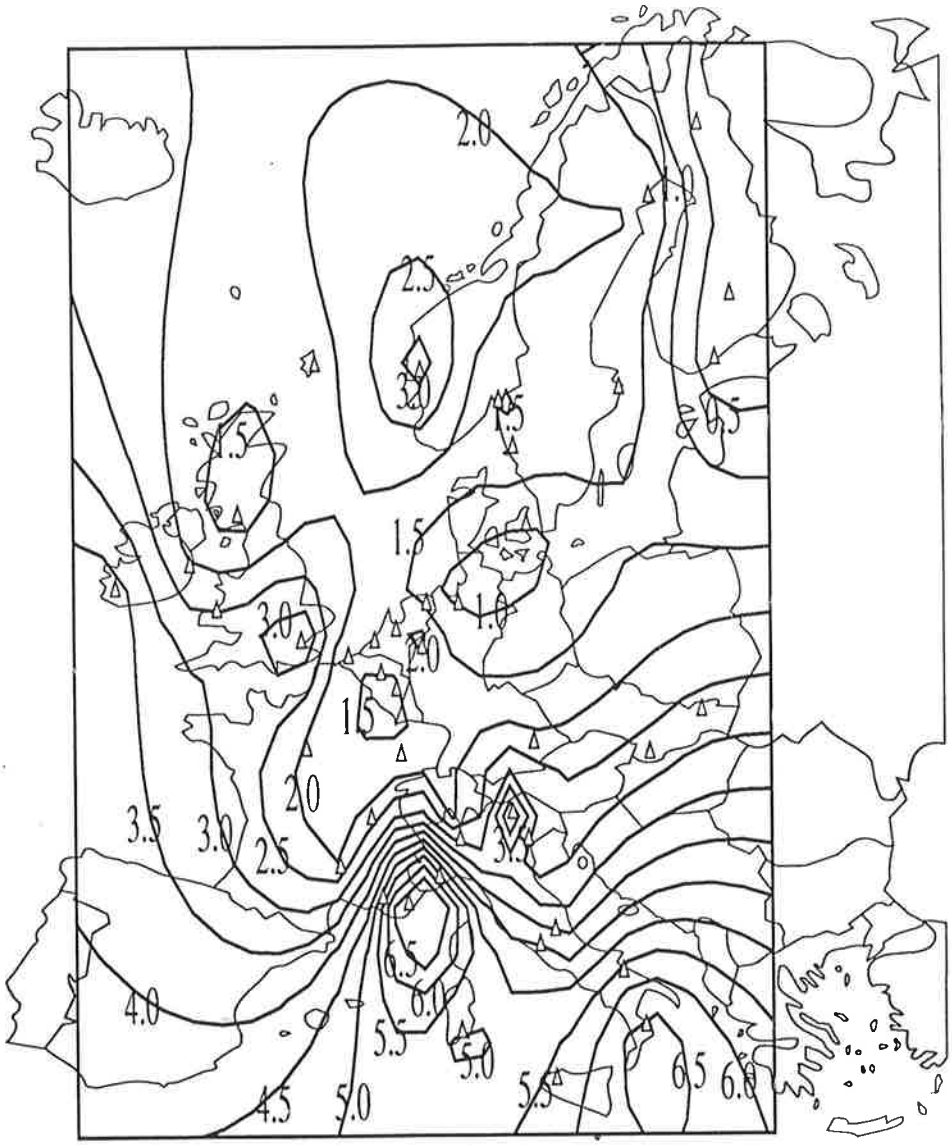

FIGURE 19 Contours of Allowable Moisture Release for the P2 Pivot in Europe

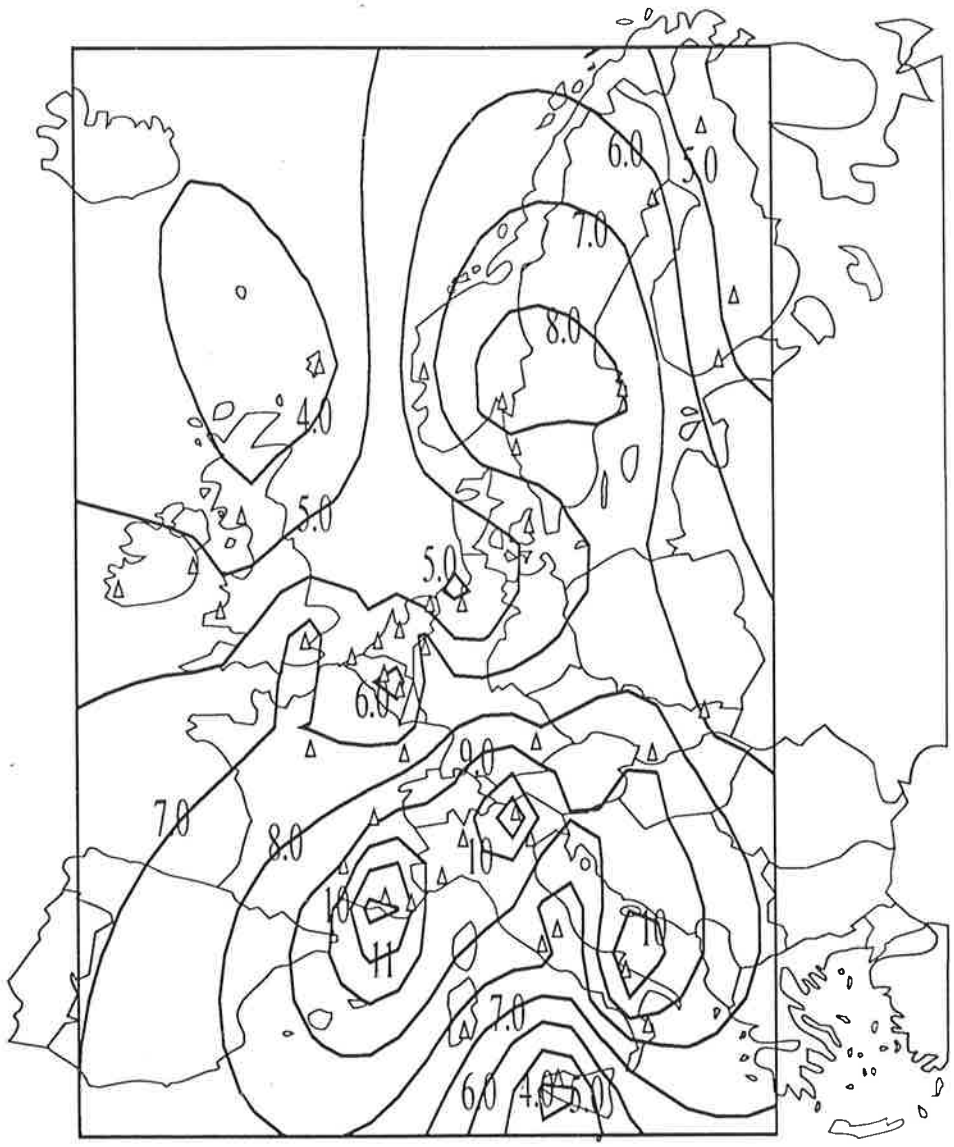

FIGURE 20 Contours of Allowable Moisture Release for the P3 Pivot in Europe

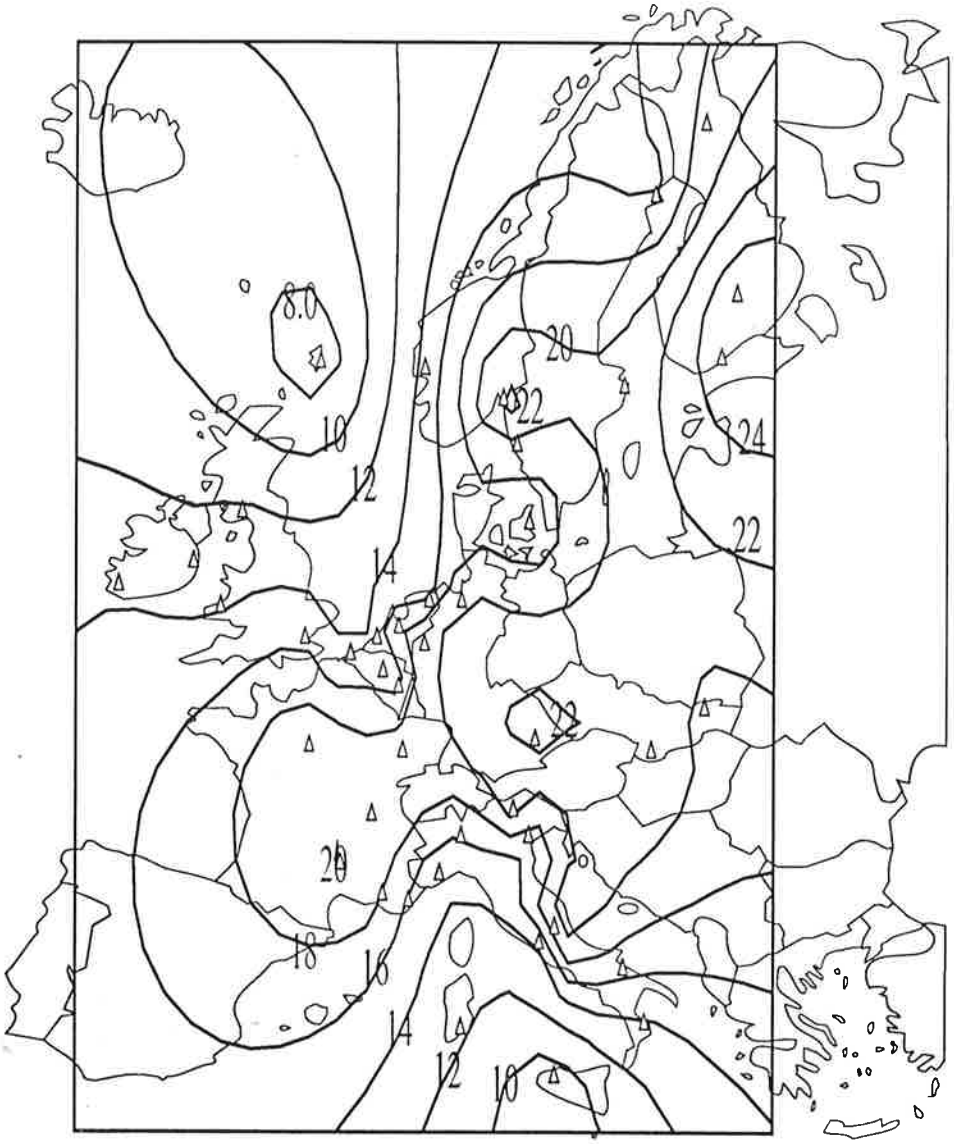

FIGURE 21 Contours of Pivot 1 for the United States and Canada

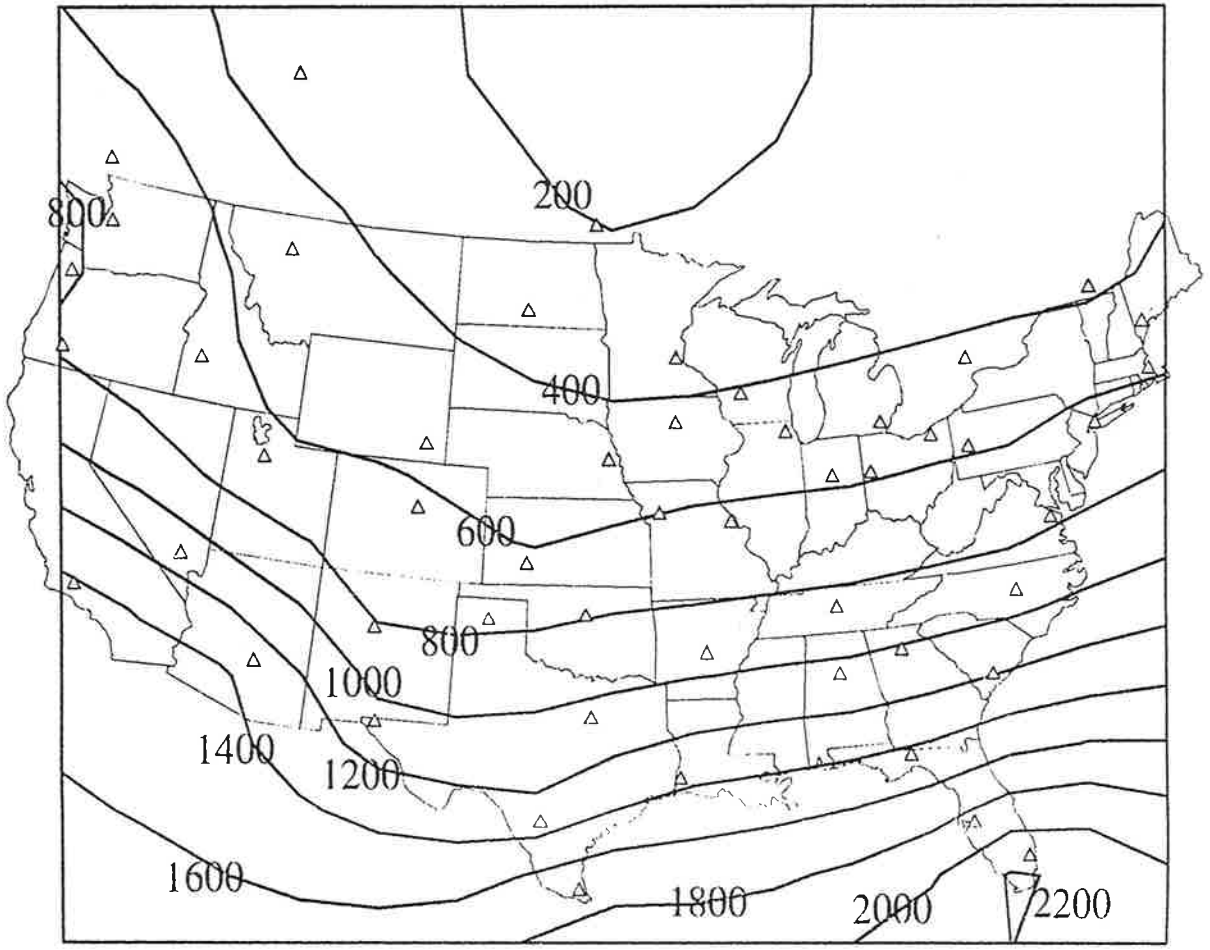

FIGURE 22 Contours of Pivot 2 for the United States and Canada

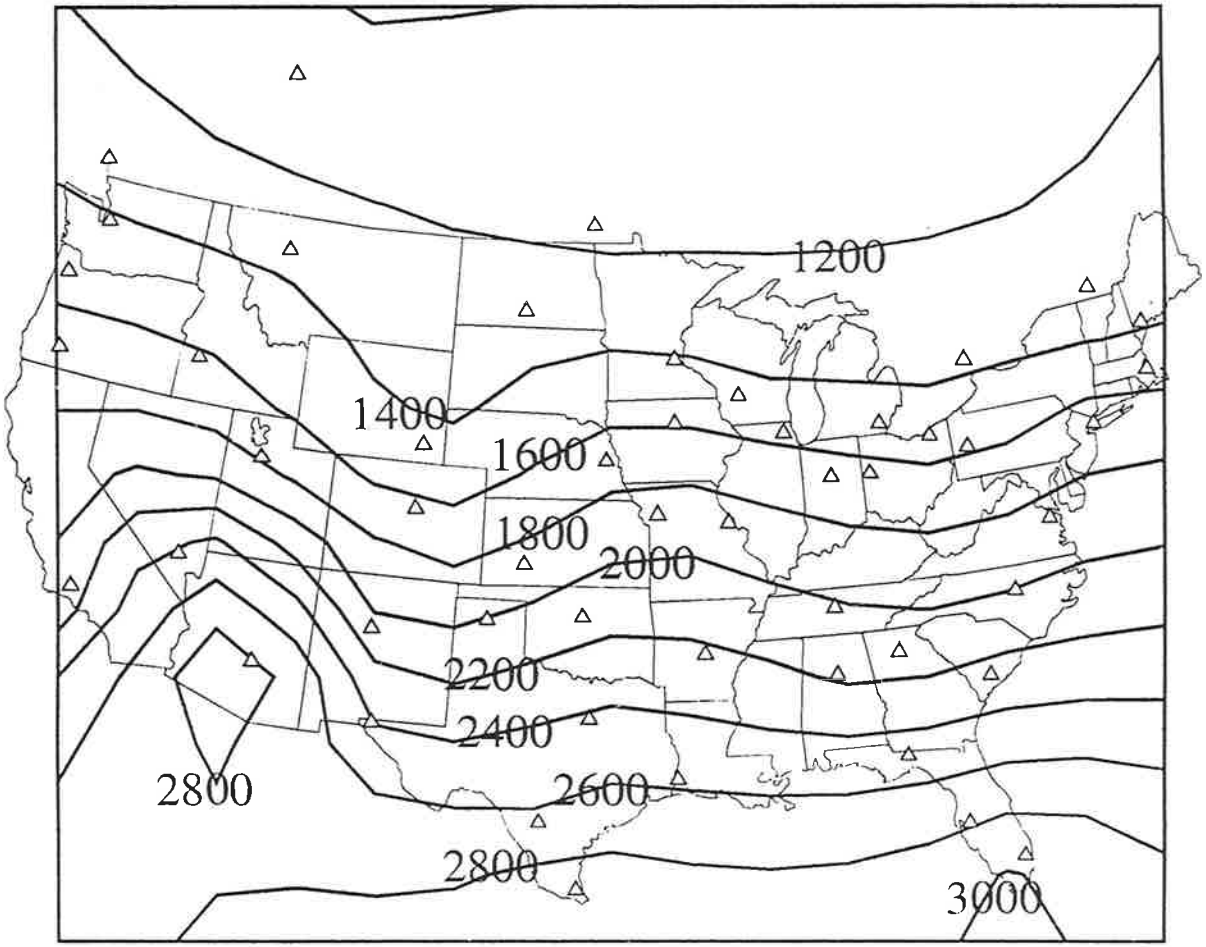

FIGURE 23 Contours of Pivot 3 for the United States and Canada

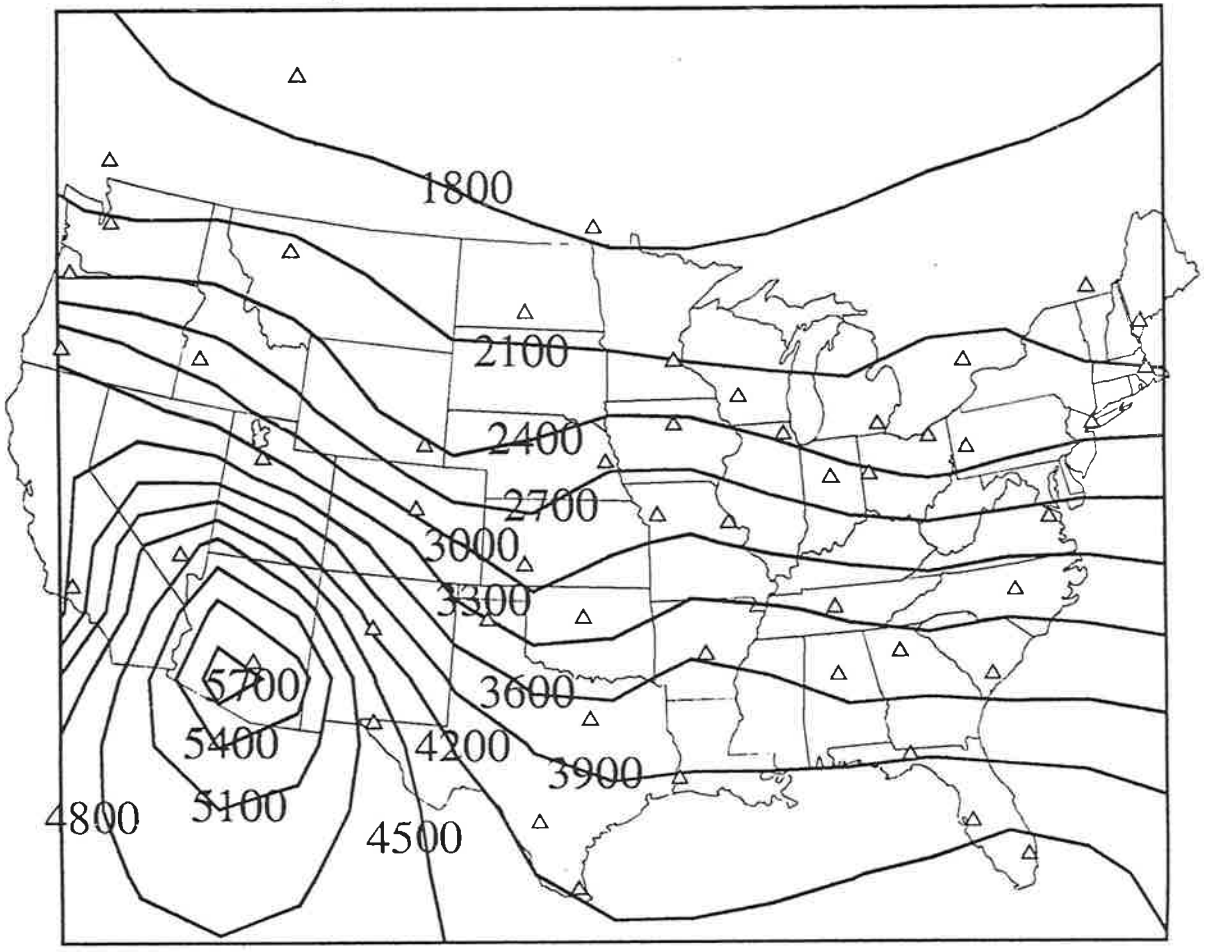

FIGURE 24 Contours of Allowable Moisture Release for the P1 Pivot in the United States and Canada

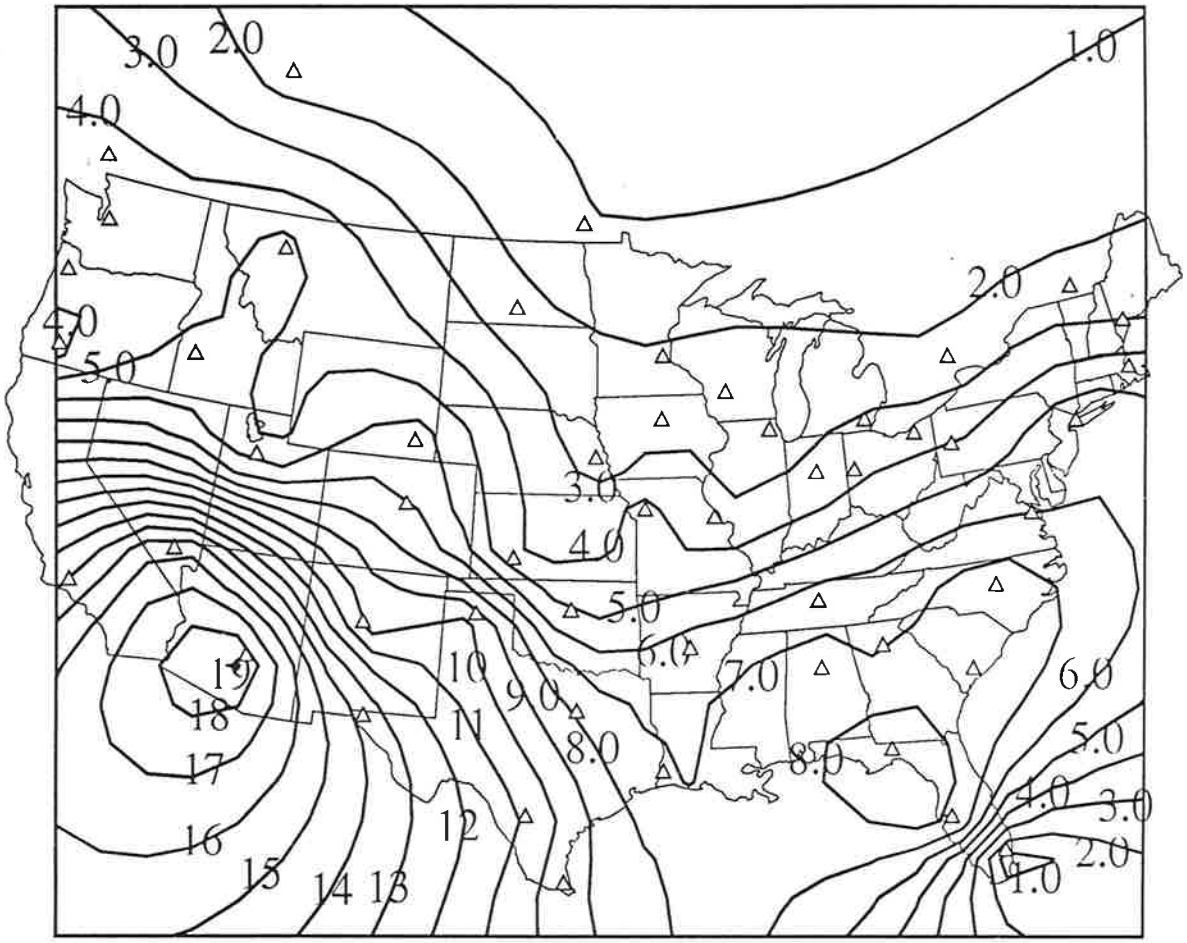

FIGURE 25 Contours of Allowable Moisture Release for the P2 Pivot in the United States and Canada

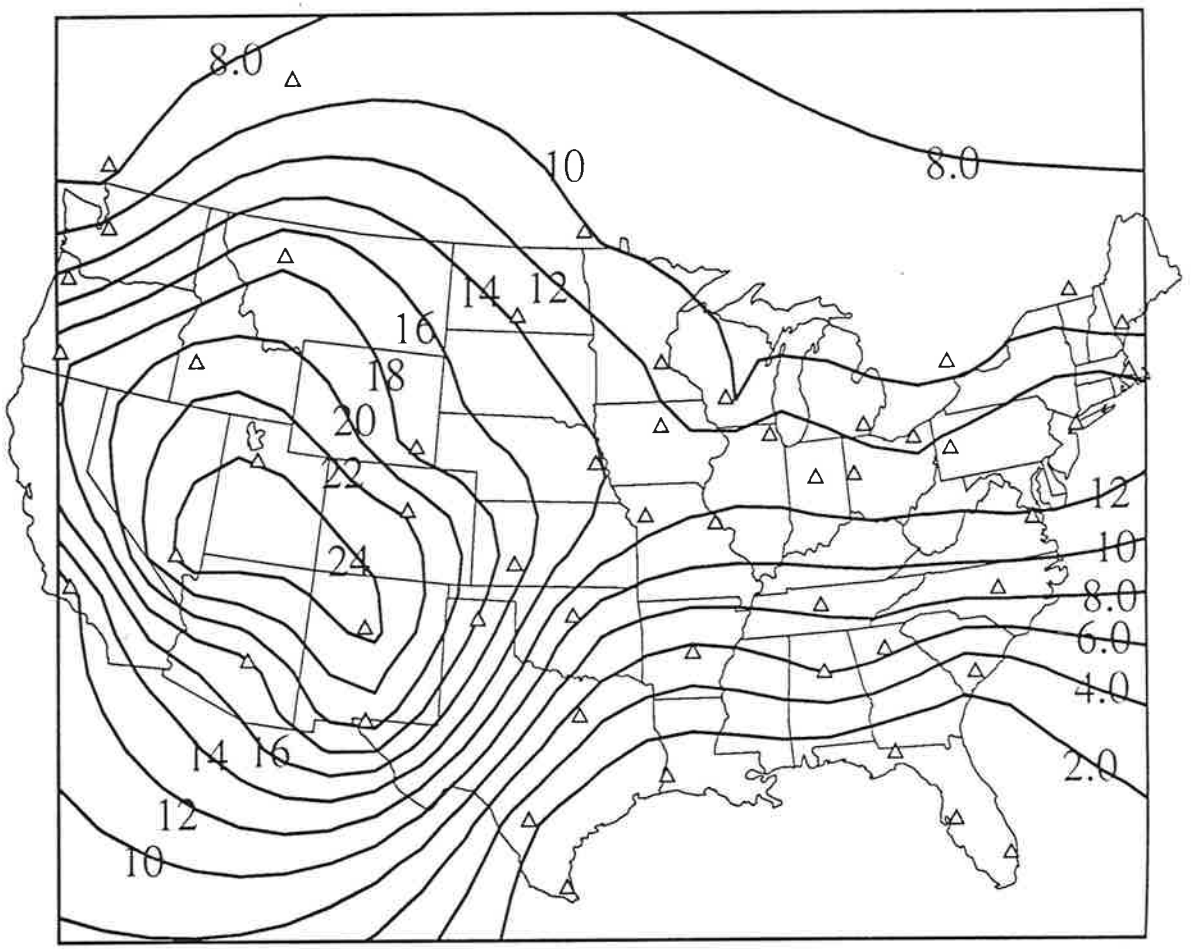

FIGURE 26 Contours of Allowable Moisture Release for the P3 Pivot in the United States and Canada

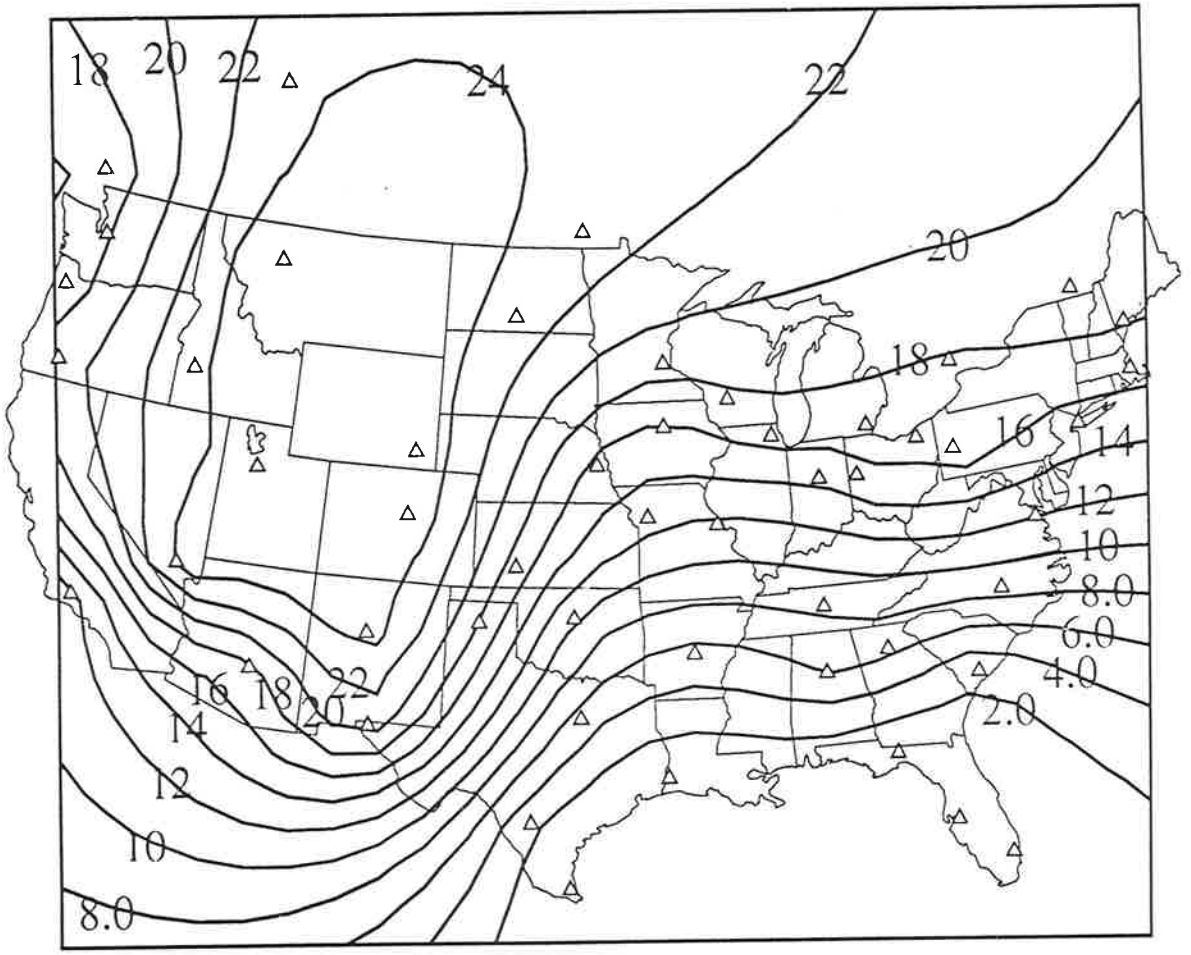

druk acco leuven - 016 / 29.11.11